Diversity and structure of fragmented populations of a threatened endemic cyprinodontid (*Aphanius sophiae*) inferred from genetics and otolith morphology: implications for conservation and management

Running title: Genetic structure in *A. sophiae* populations

Carles Alcaraz[a, ✉] and Zeinab Gholami[b, c]

[a] *IRTA Marine and Continental Waters, Carretera Poble Nou Km 5.5, E-43540 Sant Carles de la Ràpita, Catalonia, Spain.* ORCID: 0000-0002-2147-4796

[b] *Department of Biology, University of Isfahan, Isfahan, Iran*.

[c] *Department of Earth and Environmental Sciences, Palaeontology & Geobiology & GeoBio-Center LMU, Ludwig-Maximilians-University, D-80333 Munich, Germany*

✉ Corresponding author. carles.alcaraz@gmail.com // carles.alcaraz@irta.cat

Abstract

The assessment of population structure and genetic diversity is crucial for management and conservation of threatened species. Natural and artificial barriers to dispersal (i.e., gene flow) increase populations' differentiation and isolation by reducing genetic exchange and diversity. Freshwater ecosystems are highly fragmented because of human activities. Threatened species with small population sizes are more sensitive to habitat fragmentation effects. Here, we investigate the genetic population structure and gene flow among seven populations of *Aphanius sophiae* in the Kor Basin by using sequences of the complete Cyt *b* gene and otolith morphometry. The Cyt *b* gene showed low level of genetic variation, only 4.12 % of the identified sites were variable and 2.42 % were parsimony informative. Overall, haplotype diversity was low to moderate and nucleotide diversity was low to extremely low. Fish populations exhibited high levels of genetic differentiation, suggesting limited gene flow among them. These differences were obtained not only among geographically distant populations, but also among neighboring localities. Genetic population structure was supported by the AMOVA analysis, and by the haplotype network (only one of 21 haplotypes were shared by two localities). Otolith morphometric analysis was in agreement with genetic results, the two most distant and isolated populations were clearly separated, and genetically close populations showed less differences in morphometry. A significant pattern of isolation-by-distance was also detected among *A. sophiae* populations, with genetic distance more correlated with hydrological distance than with geographic distance. Results suggested that limited gene flow due to habitat fragmentation is an important factor contributing to genetic structuring and to the loss of genetic variation of *A. sophiae* populations. *Aphanius sophiae* population structure seems to be the result of habitat fragmentation and water pollution, but other factors such as introduced species should be considered. Given the high degree of genetic structuring, the definition of conservation groups is of particular importance for *A. sophiae*, which should be considered endangered according to the IUCN criteria. Conservation plans must recognize the genetic independence of populations and manage separately preventing the loss of locally adapted genotypes.

Keywords: *Isolation; Gene flow; Otolith morphometrics; Cyt b; Kor Basin*

1. INTRODUCTION

The assessment of population structure and genetic diversity is essential for both conservation and management strategies of threatened species. The amount and distribution patterns of genetic variation determine the evolutionary adaptability of populations to changing environments, and thus affecting their long-term viability (e.g., Khan & Sharma, 2010; Ouborg, Pertoldi, Loeschcke, Bijlsma, & Hedrick, 2010). Threatened species tend to have small and isolated populations, and often present a low level of genetic diversity because of genetic drift, inbreeding, bottlenecks, and founder effects (Chiari et al., 2012; González et al., 2017). These factors reduce genetic diversity and increase the genetic differentiation among populations, thus placing them at higher risk of extinction (Chung, Nason, & Chung, 2005; González et al., 2017). In freshwater ecosystems, genetic structure is mediated by the combination of natural and artificial barriers to dispersal. Natural barriers such as waterfalls, climate and hydrology alter genetic connectivity and gene flow (Fullerton et al., 2010; Faulks, Gilligan, & Beheregary, 2011; Oromi et al., 2019). Anthropogenic disturbances such as dams, flow regulation, and pollution, increase habitat fragmentation and isolation, thus reducing genetic exchange and genetic diversity (Faulks et al., 2011; Alcaraz et al., 2015*a*; Díez-del-Molino et al., 2018). Consequently, understanding genetic diversity, population structure within and among populations, spatial distribution patterns, and the presence of dispersal barriers are critical to quantify the degree of genetic exchange and to identify isolated populations (Chung et al., 2005; Bonato et al., 2018; Casal-López et al., 2018). This information is essential in designing effective habitat management and species conservation plans.

Species of the genus *Aphanius* Nardo, 1827 (Pisces: Cyprinodontidae) inhabit a wide range of habitats in the Mediterranean, Red Sea and Persian Gulf basins, including coastal marine environments and inland waters over a wide range of salinities from freshwater to hypersaline conditions (Kottelat & Freyhof, 2007; Coad, 2018). A total of 34 species are currently recognized in the genus (www.fishbase.org) from which 15 species are found in Iran (a diversity hotspot for this genus). Most of the *Aphanius* species are threatened with extinction because of human impacts and human mediated habitat changes (Coad, 2018). Identification of populations, their connectivity and the assessment of genetic diversity is of primary interest for defining conservation units, planning effective habitat management priorities, and design conservation strategies. The Kor toothcarp, *Aphanius sophiae* (Heckel, 1847), is a small cyprinodont (maximum TL < 6 cm), originally considered endemic to the Kor Basin (southwest Iran). It has been recently confirmed to be distributed in Semirom

Spring (Karun Basin) and Arjan Wetland (Helleh Basin) (Gholami, Esmaeili, & Reichenbacher, 2015). In the Kor Basin, the Kor toothcarp inhabits freshwater spring-streams and pools of varying salinity, along the river and around the Tashk and Bakhtegan hypersaline lakes (Gholami, Esmaeili, Erpenbeck, & Reichenbacher, 2014, Coad, 2018). However, toothcarp populations are imperilled and declining as a result of human activities such as water infrastructure development (e.g., dams, weirs, droughts), agricultural and irrigation expansion, water pollution, habitat alteration and loss, and the introduction of exotic species (Gholami et al., 2015; Coad, 2018). Consequently, there is an urgent need for its conservation, and hence for assessing genetic diversity, population structure, and resolve the relationships among populations. However, similar to other Iranian cyprinodonts, there are few genetic studies on *A. sophiae*, mainly focused on its taxonomy and distribution (e.g., Gholami et al., 2014, Gholami et al., 2015). In this study, we assessed the phylogenetic relationships within and among populations of *A. sophiae* population in the Kor Basin using sequences from the mitochondrial (mtDNA) cytochrome *b* (Cyt *b*) gene and otolith morphometry. Because otolith shape and morphometry reflect a combination of genetic variation and local environmental factors, otolith morphometric analysis is an efficient tool widely used for providing a phenotypic basis for fish stock differentiation (e.g., Gholami et al., 2015; Bacha et al., 2016; Teimori, Esmaeili, Hamidan, & Reichenbacher, 2018). Specific objectives of the present paper are (1) to investigate the spatial distribution patterns of genetic variation, (2) to measure connectivity and gene flow among populations, (3) to test for isolation by distance among locations, and (4) to have a better understanding of human-driven environmental changes on genetic diversity. This information is essential for formulating conservation strategies and management proposals, including toothcarp and habitat.

2. MATERIAL AND METHODS

2.1 Study area

The endorheic Kor Basin, with a catchment area of 26,440 km^2, is located in Fars province, southwestern Iran (Figure 1). The Kor River originates in the Zagros Mountains (*ca*. 4432 m above mean sea level) and flows about 280 km to the chloride Bakhtegan Lake (*ca.* 1525 m amsl). Hence, the Kor basin can be divided into two sub-basins with different hydrological regimes. The upper Kor Basin includes the drainages of the Kor River and its main tributary, the Sivand (Pulvar) River, which meet in the lower Kor River, downstream from the Doroodzan Dam (Figure 1). The watersheds of both rivers include several spring streams. The mean annual precipitation in the basin is 344 mm, ranging between 130 and 753 mm/year, and the snow cover in the Zagros Mountains maintains a stable flow throughout the year. Therefore, under natural conditions, the connection and genetic exchange between fish populations is not limited. However, the Kor River has become an important source of water for many human needs, including public supply, agriculture, industry and hydroelectric energy production (Sheykhl & Moore 2012). The construction of several dams in the basin, over the last decades (Haghighi & Kløve, 2017), has created physical barriers to fish movements and altered river flow regime, thus increasing fish populations' isolation and preventing genetic exchange between them. The recent construction of the Doroodzan Dam in 1973 and its posterior modification in the 80's is the major environmental impact on the basin. River flow regulation and water use have increased water pollution (e.g., agricultural and industrial wastewater), severe droughts, and the evaporation of the groundwater (Nadji, 1997; Sheykhl & Moore, 2012; Gholami, Teimori, Esmaeili, Schulz-Mirbach, & Reichenbacher, 2013). Consequently, the spring-streams are negatively affected by reducing average flow and increasing intermittence, and in some cases disappearing completely (Nadji, 1997; Gholami et al., 2013).

The lower Kor River (i.e., the Korbal Plain) has been historically regulated by six diversion dams (Figure1), the oldest, the uppermost Band-e-Amir dam, was built about 1000 years ago (Haghighi & Kløve, 2017). River damming, diversion and the expansion of the irrigation area and canals have drastically reduced lake inflow (Figure1), thus the two sub-basins are not always connected such as in summer and during drought periods. The Bakhtegan sub-basin includes two hypersaline lakes, the Bakhtegan and the Tashk. Lakes are characterized by shallow water depths (< 3 m), very high and variable salinity (up to 250 g/L), and variable surface area, in very wet years form a single water body with a surface area of about 1300 km^2 (Haghighi & Kløve, 2017). Both lakes are fishless, and along with the lower Kor River several isolated freshwater springs and spring-streams feed the lakes, but currently, due to man-made pollution, intensive water abstraction, and agricultural expansion most of these springs are completely dried, only Gomban and Mohammadabad Spring-streams (Figure 1) are permanent (Gholami et al., 2013; Gholami et al., 2015; Haghighi & Kløve, 2017). In rainy years, the Tashk Lake is also fed by overflow from the Kamjan Marshes (Figure 1), which are connected to the Kor River through the agricultural network. The genetic connectivity among sampled *Aphanius* populations is expected to be extremely limited, mainly between the two subsystems (i.e., the river and the lake). Rainfall allows the connection between some sites (e.g., Kamjan and Gomban), thus populations are not as isolated as they might appear and gene flow is expected.

2.2 Sample collection and mitochondrial DNA extraction

A total of 144 specimens of *Aphanius sophiae* were collected from seven localities in the Kor Basin, all corresponding to shallow spring-streams with dense aquatic vegetation (Figure 1). Fish sampling sites and samples sizes (*N*) are summarized in Table 1. Fish were captured during daylight hours in February 2012 with a fine-mesh dip net. In the field, fish were euthanized with an overdose of MS-222 (tricaine methanosulphonate), transferred to 5 % ethanol for 10 min to avoid shrinkage, and then preserved in 96 % ethanol. All specimens are deposited in the Zoological Museum of Shiraz University, Collection of Biology Department (ZM-CBSU), Iran. In addition to the newly collected specimens, 14 individuals of *A. sophiae* from the Maloosjan spring, located near the species type locality, were included in the analysis (Table 1); these are the same specimens as used in Gholami et al. (2014). Outgroups sequences from *Aphanius* sp. obtained from GenBank (National Center for Biotechnology Information, http://www.ncbi.nlm.nih.gov) were also included in the molecular genetic analysis (Supporting Information Table S1).

In the laboratory, a small piece of dorsal muscle tissue from each fish (*N* = 56) was removed under sterile condition and placed in 96-well Eppendorf PCR plates until further processing. Total genomic DNA was isolated and purified using selective binding to a fiberglass membrane (AcroPrep 1 µM glass fiber; Pall 5051) in the presence of high concentration of Guanidinium Thiocyanate (GITC) following the procedures outlined in Vargas et al. (2012). The entire cytochrome *b* gene was amplified from total genomic DNA using the Polymerase Chain Reaction (PCR) with universal primers L14724, 5'-GTGACTTGAAAAACCACCGTTG-3', and H15915, 5'-CAACGATCTCCGGTTTAGAAGAC-3' (Irwin, Kocher, & Wilson, 1991), and previously used in *Aphanius* studies with satisfactory results (e.g., Perdices, Carmona, Fernández-Delgado, & Doadrio, 2001; Gholami et al., 2014). PCR amplification was performed under the following conditions: 92 ºC for 3 min and then 34 cycles at 92 ºC for 1 min, 53 ºC for 90 sec, and 72 ºC for 3 min. At the end of the 34 cycles, the reaction mixture was incubated for an additional 4 min at 72 °C. PCR products (amplicon size ∼1220 bp) were purified with the PEG (Polyethylene Glycol) protocol as described in Rosenthal et al. (1993). PCR-amplified and cleaned DNA were bidirectionally sequenced by using BigDye 3.1 Terminator Cycle Sequencing (Applied Biosystems, Munich, Germany) on an ABI 3730XL automated sequencer at the Genomic Sequencing Unit, Department of Biology, LMU, Munich. Dye terminator cycle sequencing was performed following the protocol provided by the manufacturer, with the same primers used for amplification, i.e. 96 ºC for 1 min (preincubation) followed by 30 cycles of denaturation (96 ºC for 15 seconds), annealing (52 ºC for 10 min), and extension (60 ºC for 90 seconds). The resulting DNA sequences were assembled, edited and aligned by using the default settings in Geneious 6.4 (http://www.geneious.com). The obtained cytochrome *b* sequences of the studied *Aphanius* populations have been deposited in GenBank, accession numbers from KJ634159 to KJ634206 (Table 1).

2.3 Phylogenetic, genetic diversity and gene flow analyses

Maximum likelihood phylogenetic trees were generated by using the PhyML algorithm available in SeaView 4 (http://doua.prabi.fr/software/seaview). The best fitting nucleotide substitution model (GTR + G) and its parameter values were determined by Akaike Information Criterion (AIC) implemented in jModelTest 2.1.1. Phylogenetic relationships were also estimated by Bayesian inference (BI) analyses based on Markov Chain Monte Carlo (MCMC) algorithms using MrBayes 3.2 (http://mrbayes.sourceforge.net/). Bayesian inference analyses consisted of two independent runs of four MCMC chains with $2{\times}10^6$ generations each, under the most generalized model (GTR + G + I) because overparameterization does not negatively affect Bayesian analyses (Huelsenbeck & Ranala, 2004). Convergence was achieved when the final standard deviation for the split frequency was < 0.01, and the likelihood values of the sampled trees from both runs reached a stationary distribution. The first 25 % of trees were discarded as burn-in. The Fu's F_S (Fu, 1997), Tajima's D (Tajima, 1989) and the R_2 (Ramos-Onsins & Rozas, 2002) neutrality tests were calculated with DnaSP 6.11.01 (http://www.ub.edu/dnasp/) to differentiate models of population growth from the null hypothesis of a constant population size under the neutral model, i.e. to test past for population changes and/or deviations from neutrality. The significance of the neutrality tests was determined based on 1000 coalescent simulations. Both F_S and R_2 neutrality tests are the most powerful tests for detecting sudden population growth or contraction, but while F_S is recommended for large population sizes, R_2 is the most sensitive for small ones (Ramos-Onsins & Rozas, 2002). Global and between populations pairwise F_{ST} values were also calculated to assess gene flow and to estimate the degree of genetic connectivity. Pairwise F_{ST} values were calculated in Arlequin 3.5.2.2 (http://cmpg.unibe.ch/software/arlequin35/), the statistical significance was determined by 1000 permutations followed by Bonferroni correction for multiple comparisons. A haplotype network was constructed with TCS 1.21 (http://darwin.uvigo.es/software/tcs.html) using the statistical parsimony method (Templeton, Crandall, & Sing, 1992). This method estimates an unrooted tree and provides a 95 % plausible set of the relationships among haplotypes. A hierarchical analysis of molecular variance (AMOVA) was carried out with Arlequin 3.5.2.2, using the groupings suggested by phylogenetic tree and haplotype network analysis, and the different regions according to geographic localization. AMOVA quantifies the genetic variation at three levels: among groups, among populations within groups, and within populations; the statistical significance was assessed using 9,999 permutations. The degree of isolation by distance (IBD) among populations was tested using a Mantel test (10,000 permutations) between linearized genetic and geographic distance matrices, with IBDWS 3.23 (http://ibdws.sdsu.edu/~ibdws/). Genetic diversity was also evaluated by nucleotide diversity (π), haplotype diversity (H) and nucleotide polymorphism (θ).

2.4 Otolith morphology and statistical analyses

Variations in size and shape of the saccular otolith (sagitta) are used in the discrimination of fish populations. In *Aphanius*, otolith morphometry is mainly genetically determined and is little influenced by habitat features, thus, is a useful indicator of population differentiation (e.g., Reichenbacher, Sienknecht, Küchenoff, & Fenske, 2007; Reichenbacher, Feulner, Schulz-Mirbach, 2009). Hereafter, 'otolith' refers to the saccular otolith. Fish skulls (N = 144) were opened dorsally and right and left otoliths were removed, cleaned of adherent tissue by incubation in 1 % potassium hydroxide (KOH) solution for 3-4 h, rinsed in distilled water for 4–5 h, and finally washed several times, following the procedures described in Reichenbacher et al. (2007). Morphology was studied using a stereomicroscope and scanning electron microscopy (LEO 1430 VP) (Figure 2). Digital images from the left otoliths were captured with a Leica DFC 295 camera for morphometric analysis, three angles and eight linear distances were measured directly using the Leica Image Software (IMAGIC 1000), and eight morphometric variables were derived from these (Figure 2, Supporting Information Table S2). Differences in morphometric variables among fish populations were first analyzed with multiple analysis of covariance (two-way MANCOVA), using standard length as covariate (see Rovira, Alcaraz, & Ibáñez, (2012) for more details). In addition to P values, we used η^2 (eta squared) as a measure of effect size (i.e. importance of factors). Similarly to the regression coefficient (r^2), η^2 is the proportion of variation explained for a certain effect (see Alcaraz, Pou-Rovira, & García-Berthou, 2008*a*; Alcaraz, Gholami, Esmaeli, & García-Berthou, 2015*b* for more details). Stepwise forward canonical discriminant analysis (CDA) was performed considering otolith morphometric variables and fish standard length in order to find linear combinations of the variables that best summarized differences among fish populations. Males and females were merged for the statistical analyses increase statistical power and interpretability. All statistical analyses were performed with SPSS 24.0.

3. RESULTS

3.1 Genetic diversity and structure

A total 1,153 bp segment of Cyt *b* was obtained for 56 individuals of *Aphanius sophiae* collected from seven localities in the Kor Basin (Figure 1), including 8 sequences from the study by Gholami et al. (2014). After correction and alignment, a matrix of 825 bp consensus Cyt *b* sequences was obtained (see fasta file as Supporting Information). The average nucleotide composition of the Cyt *b* sequences was A = 25.1 %, T = 32.15 %, C = 27.03 %, and G = 15.61 %, with a bias against G and consequently in GC content (42.64 %). Overall, both the Tajima's *D* and Fu's *Fs* neutrality tests showed significant negative values (Table 2), thus indicating deviation from neutrality due to an excess of rare alleles as would be expected from a recent population expansion (e.g., after a bottleneck) or from genetic hitchhiking (i.e., positive selection). Similarly, R_2 statistic (R_2 = 0.069, P < 0.01) showed a small positive value, again indicating population growth.

Among the seven *Aphanius* populations, *H* varied between 0 and 1, π ranged from 0 to 0.0055, and *k* ranged from 0 to 4.5357 (Table 2). For all the estimated genetic indices, Safashahr and Mohammadabad were the least variable populations with all the individuals from the same population sharing the same haplotype, and the highest levels of both *H* and π were observed for Kamjan and Gomban, where all sequenced individuals had unique haplotypes (Table 2). Overall, most of the haplotypes were unique to their own population. Of the 21 unique haplotypes identified in the 56 individuals examined, no haplotype was shared between two geographical localities, with the exception of one haplotype that was shared between the neighboring Denjan and Maloosjan (Figure 1, Table 2), found in six and two individuals respectively. Tajima's *D* and Fu's *Fs* were all non-significant (except for Gomban), albeit negative for Denjan and Kamjan, as expected for a recent population expansion or selection (Table 2). Positive values were obtained for Safashahr and Maloosjan, thus suggesting a recent bottleneck.

3.2 Phylogeographic relationships and gene flow

We additionally obtained 23 sequences of the Cyt *b* from nine *Aphanius* species (Supporting Information Table S1), which were combined with the molecular Cyt *b* matrix and used as outgroup in the phylogenetic tree construction. Phylogenetic analysis was performed by two independent methods, i.e. maximum likelihood (ML) and Bayesian inference methods (BI). Phylogenetic analyses were largely congruent, with both methods producing similar tree topologies and identical relationships among *A. sophiae* populations (Figure 3). However, although ML and BI analysis supported the same tree topology, ML bootstrap values were lower when compared to those obtained by BI (Figure 3). Based on the phylogenetic tree typology the geographically closer Denjan and Maloosjan fish populations were mixed together forming a monophyletic lineage (Posterior P > 0.95). Individuals from Safashahr, Mohammadabad and Ghadamgah populations formed three distinct monophyletic lineages (Posterior P > 0.95, in the three populations) identified by three geographically and phylogenetically different haplogroups, thus representing a high degree of population isolation (Figure 1, Figure 3). Finally, there was some overlap among individuals from Gomban and Kamjan populations, and with some individuals distributed in the basal node defining the relationship among fish populations (Figure 3). Consequently, phylogenetic analysis suggested a highly significant geographical structuring in *A. sophiae* populations from the Kor Basin, which is well in accordance with their geographical distributions and the historical impact of river barriers. The result of the haplotype network showing the relationship and the distribution of haplotypes was also consistent with the phylogenetic tree (Figure 3, Figure 4). There was a clear structuring by geographic origin of *A. sophiae* populations from the Kor Basin. Most of the haplotypes were only present in one population and occurred as independent branches of one or two haplotypes connected to the core haplotype (Hap 1) by few mutations, usually a single or two mutations steps (Figure 4). Haplotypes from both Gomban and Kamjan populations did not show an evident structure, most of the mutations were from Gomban to Kamjan haplotypes but Gomban haplotype 6 mutated from Kamjan haplotype 5 (Figure 4).

Genetic structuring by geography was further confirmed by pairwise genetic distance (F_{ST}) analysis, a measure of population divergence that ranges from 0 (similar polymorphisms) to 1 (high level of divergence between populations). The global estimate of F_{ST} across all *A. sophiae* populations was significantly different from zero (F_{ST} = 0.7613, P < 0.0001), indicating significant genetic differentiation among the seven populations. The mean pairwise F_{ST} value was 0.7308 (SE = 0.0510), thus showing an extremely high level of genetic structuring. Furthermore, all of the pairwise F_{ST} values were high and significant, thus showing the restricted gene flow among these populations and the high level of genetic differentiation between populations (Table 3). Only the pairwise F_{ST} value obtained between Kamjan and Gomban populations was not significant (Table 3), thus suggesting a high level of gene flow and low genetic structure between them. A significant positive correlation was obtained between hydrological (Supporting Information Table S4) and genetic distances (Mantel test; *r* = 0.69, *P* = 0.001), thus confirming that populations of *A. sophiae* in the Kor Basin are in isolation by distance. A significant correlation was also detected when Safashahr (*r* = 0.71, *P* = 0.001) and Mohammadabad (*r* = 0.65, *P* = 0.012), the farthest populations (Figure 1), were not included in the analysis.

The AMOVA conducted without grouping showed high and significant levels of genetic structure among *Aphanius* populations, since most of the variation was explained by differences among populations (Table 4). Therefore, we also tested for large-scale patterns of genetic structure with AMOVA, considering three grouping options (Table 4). First, the seven *A. sophiae* populations were grouped based on sub-basin drainage system (i.e., the upper and the lower Kor Basin, see methods). Second, all sampled populations were divided in three groups: 1) populations from the lower Kor Basin; 2) the two uppermost populations (i.e., Safashahr and Ghadamgah); and 3) Denjan and Maloosjan populations. Third, all sampled populations were grouped based on clusters identified by both phylogenetic and analysis and haplotype network (Table 4). AMOVA identified significant genetic structure at all the hierarchical levels examined. In the first option, the greatest proportion of the overall variation was accounted for among populations within groups. However, in the latter two options, AMOVA showed that dividing sampled populations into groups based on the geographic distribution significantly reflected genetic structuring (Table 4), with the largest amount of the total variation explained by the among groups diversity. Therefore, results suggest significant geographical structure in *A. sophiae* populations, thus coinciding with the constructed river barriers and human alteration of the river network, including the river floodplain system.

3.3 Otolith morphometrics and differences among populations

Individuals were categorized in four size (i.e., standard length) groups, with two of the four size classes ($20 < SL \leq 27$ and $27 < SL \leq 35$ groups) displaying otolith morphometric information for all populations (Supporting Information Table S5). The largest otolith length-standard length ratios were found in Mohammadabad, while the smallest ratios were recorded in Safashahr (Supporting Information Table S5). Overall, *A. sophiae* otoliths presented a straight sulcus covered by several colliculi, with an ostium ovate to rounded and shorter than the cauda (Supporting Information Figure S1). In otoliths from Safashahr, Maloosjan and Mohammadabad the ostium was usually opened to the anterior margin, but in Ghadamgah, Denjan, Kamjan and Gomban the ostium may be either opened or closed. Otoliths from Safashahr exhibited a quadrangular to rounded-triangular shape with a highly variable excisura angle. The rostrum was rounded and rather developed than the antirostrum, which was slightly shorter. The dorsal margin was smoothly curved and the posterior rim was steep (Supporting Information Figure S1). In Ghadamgah, Denjan, Maloosjan, Kamjan, Gomban and Mohammadabad otoliths showed a well-developed rostrum (often forming a prominent pointed-tip) and antirostrum (usually rounded-tip); but the rostrum was clearly longer, especially in Mohammadabad. The excisura angle was mainly V- or U-shaped. The dorsal margin was curved, but wrinkled in Mohammadabad; the posterior rim was steep, and a prominent posteroventral edge was present in Mohammadabad and in some individuals from Denjan and Gomban. Overall, otoliths were rounded-triangular or trapezoid shaped, only in Gomban triangular shape were identified (Supporting Information Figure S1).

After accounting for fish length (MANCOVA, Wilks's $\lambda = 0.182$, $F_{18, 119} = 29.69$; $P < 0.001$; $\eta^2 = 0.82$) otolith morphometric variables differed significantly among populations (Wilks's $\lambda = 0.182$, $F_{108, 689.17} = 29.69$; $P < 0.001$; $\eta^2 = 0.68$). Univariate tests confirmed this pattern (Figure 5, Supporting Information Figure S2). Only two morphometric variables (i.e., posteroventral angle and relative rostrum height) did not show significant differences among populations ($P > 0.24$). Overall, the most variables with the greatest importance (power analysis, η^2) differentiated three groups; Safashahr, Mohammadabad and one composed by Ghadamgah, Denjan, Maloosjan, Kamjan, and Gomban (Figure 5). Usually, fish from Safashahr had the smallest morphometric characters (e.g., dorsal part length, maximum height and length, medial part length and rostrum length), while fish from Mohammadabad showed the largest values (Figure 5, Supporting Information Tables S6 & S7). Similar results were obtained when only SC2 and SC3 fish groups (Supporting Information Table S5) were considered. The stepwise discriminant analysis used to select otolith morphometric characters that best discriminated among the seven *A. sophiae* populations supported previous findings. Nine variables were retained in the stepwise CDA; medial part length, fish standard length, relative antirostrum length, maximum length, dorsal part length, maximum length-maximum height index, antirostrum length and excisura angle. The overall percentage of correct classification was 77.1 %, with the first two discriminant functions explaining 80.4 % of the total variation (62.7 and 17.7 %, respectively) observed among populations. The CDA revealed a clear separation of Safashahr and Mohammadabad (Figure 6), with an accuracy of 100 % for both populations (Table 5). The results also showed that otoliths can be assigned to Ghadamgah, Kamjan and Gomban populations with accuracies over 70 % (Table 5).

4. DISCUSSION

4.1. Genetic variation

Together with historical events, population-level genetic structure across species geographic range is influenced by current processes, such as gene flow, selective force heterogeneity and genetic drift (Chiari et al., 2012; González et al., 2017). The Cyt *b* gene (mtDNA) showed low level of genetic variation, only 4.12 % of the identified sites were variable and 2.42 % were parsimony informative. Such degree of genetic variability and nucleotide diversity (π = 0.0061) are lower or similar than those reported, using the same molecular genetic marker, for other threatened freshwater fish species with larger geographic ranges (e.g., Buonerba et al., 2015), cyprinodontid (e.g., Marchio & Piller, 2013), and *Aphanius* (e.g., Chiozzi et al. 2017; González et al., 2017). Within *A. sophiae* populations, haplotype diversity was low to moderate, except in Kamjan and Gomban, and nucleotide diversity was low to extremely low. Safashahr and Mohammadabad, the two most distant and isolated populations, had the lowest values for both haplotype and nucleotide diversity indices.

The low degree of genetic diversity observed within *A. sophiae* populations could be the result of founder effects. Both the low values of nucleotide diversity and low to moderate haplotype diversity could be the result of a recent population expansion after a founder event or a bottleneck (Gutiérrez-Rodríguez, Morris, Dubois, & Queiroz, 2007), but Tajima's *D* and Fu's *Fs* values would suggest this is not case since all populations (except in Gomban) were not significantly different from 0. Consequently, the observed pattern in genetic variation is most likely the result of recent genetic drift and inbreeding process due to small population sizes and isolation (Gutiérrez-Rodríguez et al., 2007, González et al., 2017). The high haplotype diversity in Gomban and Kamjan may indicate a recent population expansion after a low effective population size, such as variation in habitat suitability during and after a severe drought. An increasing number of species are currently subjected to reductions in population size as a consequence of human activities. The Kor Basin has been historically impacted by human activities, such as industry, agriculture, damming, and channelization (Sheykhi & Moore, 2012; Haghighi & Kløve, 2017). Human impacts may have detrimental effects on fish populations, cause habitat loss, fragmentation, and prevent upstream connection (e.g., Faulks et al., 2011; Alcaraz *et al*., 2015*a*; Díez-del-Molino et al., 2018), thus reducing fish population sizes and explaining the genetic diversity within populations.

4.2. Population structure, gene flow and habitat fragmentation

The Kor Basin populations of the killifish *Aphanius sophiae* examined in this study exhibited high levels of genetic differentiation among localities both at basin and sub basin scale, thus suggesting limited gene flow among these populations. Such differences were observed not only among geographically distant populations, but also among neighboring localities. Population structure was supported by the significance of the AMOVA analysis. The AMOVA performed without grouping showed that 77.4 % of the total variation was explained by differences among population, and in the AMOVA with sub-basin grouping, 69.5 % of the total variation were explained by variation among populations within sub-basins, demonstrating the high genetic differentiation among fish populations from the same sub-basin. These results were also supported by the haplotype network, as only one haplotype out of 21 were shared by two localities (Denjan and Maloosjan), and the high and significant F_{ST} values between all pairs of populations (except between Kamjan and Gomban). Otolith morphometric analysis was concordant with the population genetic structure. *Aphanius* otolith morphometry is little influenced by habitat features and differences are mainly genetically determined, thus being a useful indicator of population differentiation (Reichenbacher et al., 2009). Overall, fish from Safashahr exhibited the smallest otoliths (after accounting for fish length) with a quadrangular to rounded-triangular shape characterized by short and rounded rostrum. Otoliths from the other fish populations were rounded-triangular or trapezoid shaped, except in Gomban where a triangular shape were identified, and showed a well-developed rostrum and antirostrum, mainly in Mohammadabad where the largest (after accounting for fish length) otoliths were found. Our results showed significant differences in otolith shape and morphology, only two of the nineteen measured morphometric characters (i.e., posteroventral angle and relative rostrum height) did not show significant differences among *Aphanius* populations. Morphometric analyses clearly separated the two most distant and isolated populations, and genetically close populations showed less differences in otolith morphometry. Overall, the classification rate by the nine variables retained in the stepwise CDA was 77.1 % and the first two discriminant functions explained 80.4 % of the total variation among populations; thus suggesting that otolith morphology reflects a high level of genetic diversity and isolation within and among *A. sophiae* populations across the Kor Basin. A significant pattern of isolation-by-distance was detected among *A. sophiae* populations. Genetic distance was more correlated with hydrological than with geographic distance (r = 0.50) suggesting that gene differentiation is more influenced by gene flow along the river axis. This discontinuity pattern is consequence of limited dispersal across space, and it might indicate barriers to dispersal. A geographic effect on genetic differentiation also resulted from the AMOVA performed on three and five groups showing that a significant amount of the total genetic variation was due to differences among geographic groups. These results suggests that gene flow may be an important factor contributing to genetic differentiation, and the potential loss of genetic variation resulting from habitat fragmentation.

F_{ST} value > 0.25 indicates “very great” (Wright, 1978) levels of differentiation between populations, and are common in species inhabiting unconnected habitats with limited gene flow between populations (e.g., Gutiérrez-Rodríguez et al., 2007). The global (0.76) and mean (0.73) F_{ST} values between all populations are among the highest values reported for freshwater cyprinodontids (e.g., Gutiérrez-Rodríguez et al., 2007; Li, Bessert, Macrander, & Orti, 2009), and are similar or even larger than those estimated for *Aphanius* species inhabiting isolated habitats, such as coastal lagoons were where gene flow is limited or absent (e.g., González, Pedraza-Lara, & Doadrio, 2014; González et al., 2017). High F_{ST} values (i.e., differentiation) can be due to low gene flow, high genetic drift or spatially variable selection (Cabe & Alstad, 1994; Buonerba et al., 2015). Although the limited dispersal ability of *A. sophiae*, gene flow between populations is likely to occur under natural conditions. The Kor River and its main tributary the Sivand River are perennial because snow melt and rainfall, thus there is a continuous river flow throughout the year (Nadji, 1997) maintaining the connectivity between populations. Under unregulated flow conditions floods are more frequent and severe, connecting the river longitudinally and to its floodplain (Ai, Sandoval-Solis, Dahlke, & Lane, 2015) allowing the genetic exchange between widely separated populations. However, the increase in water demand and the development of water infrastructure such as dams and river channelization, prevents upstream connection and modifies the natural flow regime reducing flow variability and hence frequency and duration of floods (Faulks et al., 2011; Alcaraz et al., 2015*a*; Ai et al., 2015). The resulting habitat fragmentation may reduce the size of fish populations and increases the spatial isolation, thus reducing within population genetic diversity and increasing between population genetic divergence due to elevated genetic drift and inbreeding, and diminished gene flow (Young, Boyle, & Brown, 1996; Li et al., 2009; González et al., 2017). The magnitude of the effect of habitat fragmentation on genetic differentiation may also be positively influenced by other human disturbances such as water pollution. Our results are in agreement with this pattern. Overall, F_{ST} values showed a weak but clear gradient of genetic connectivity along the fluvial axis from upstream to downstream. Safashahr and Mohammadabad were the most isolated and differentiated populations likely due the presence of artificial barriers, flow regulation and reduction. The Doroodzan Reservoir (990 hm^3) feeds the Doroodzan and the Korbal irrigation system with a potential irrigated area of 1120 km^2 (Nafarzadegan, Vagharfard, Nikoo, &

Nohegar, 2018). The development of the irrigation system in the Korbal Plain and river flow regulation have undergone a large reduction in lake area (i.e., Bakhtegan and Tashk) and most of the wetlands have completely dried out, thus preventing the connection between the springs surrounding the lakes during heavy rain periods and flood events (Nadji, 1997; Sheykhi & Moore, 2012; Gholami et al., 2013). Denjan and Maloosjan (F_{ST} = 0.39) are located in the Doroodzan irrigation system, thus restricted gene flow is possible through the channel network. F_{ST} (0.08) did not show significant differences between Kamjan and Gomban, both spring-streams are close and connected by the Korbal irrigation network and Kamjan Marshes receives the overflow from Gomban in rainy years, increasing the migration rate and genetic exchange from Gomban to Kamjan.

Although genetic and morphometric analyses were in agreement, more data (i.e., nuclear markers) are needed to confirm and complete our results. For instance, selective sweeps could also result in low heterozygosity and even in strongly differentiated populations, if local adaptation is occurring (Li et al., 2009; Angeletti et al., 2017; González et al., 2017). Altogether, our results suggest that the strong genetic structure of *Aphanius sophiae* populations from the Kor Basin is the result of population isolation due to habitat fragmentation, one of the main factors limiting gene flow between populations (Young et al., 1996). Under conditions of limited gene flow, genetic drift is probably playing an important role in population genetic differentiation, particularly because of the small effective population sizes caused by human impacts. *Aphanius* species exhibit high phenotypic plasticity and are capable of adapting to a wide range of environmental conditions (Angeletti, Cimmarauta, & Nascetti, 2010; Angeletti et al., 2017; González et al., 2017). Consequently, divergent selection pressure driven by the change in local environmental conditions and the increase in extreme conditions, such as droughts and pollution, resulted in intensified genetic drift and genetic structure of *A. sophiae* populations. Genetic drift reduces genetic diversity within populations and increases genetic differentiation between populations, leading a global reduction of the species genetic diversity. Similar genetic patterns have been also detected between populations of cyprinodontid species inhabiting naturally or artificially fragmented habitats (Li et al., 2009; González et al., 2017), and a rapid genetic loss in response to habitat degradation and changes in environmental conditions has been reported in *A.* fasciatus (Maltagliati & Camili, 2000, Angeletti et al., 2010).

4.3. Conservation and management implications

Effective management and conservation programs require knowledge of species genetic diversity, population structure, and the mediating factors. Habitat fragmentation and restricted migration increase population divergences and reduce genetic diversity within populations, genetic erosion is faster in small population and in extreme situations may result in the extinction of local populations (Young et al., 1996; Li et al., 2009). Although more data are needed, our results suggests that the current distribution of *Aphanius sophiae* in the Kor Basin is highly restricted into small populations and areas, largely isolated from each other and widely separated. The situation may be critical, the genetic pattern exhibited by *A. sophiae*, particularly the high degree of population differentiation and low genetic diversity within populations is similar to those reported for endangered *Aphanius* species (González et al., 2014, 2017). *Aphanius sophiae* is not listed on the Red List of endangered species by the International Union for Conservation of Nature (IUCN) because the limited data available. Therefore, we propose that *A. sophiae* should be included in the IUCN Red List as VU (vulnerable) or EN (endangered) according to the criteria A2ce+B1ab (ii, iii, iv); suspected population size reduction of ≥ 30-50 % over the last 10 years (A2), based on a decline in area of occupancy and quality of habitat (c), and the effects of introduced taxa, pollutants and competitors (e). Extent of occurrence estimated to be less than 5,000 km^2 (B1), populations are severely fragmented (a) and there is a decline (b) in the area of occupancy (ii), area, extent and/or quality of habitat (iii), and the number of locations (iv).

Aphanius sophiae population structure seems to be primarily the result of habitat fragmentation and water pollution, but other factors should probably be considered as well, for instance the impact of introduced species competing for the same ecological niche, such as *Gambusia holbrooki* (Alcaraz & García-Berthou, 2007; Alcaraz, Bisazza, & García-Berthou, 2008*b*), which is widely distributed in Iranian basins. Unfortunately, our results lack of demographic data, thus future studies should combine genetic and demographic parameters such as density, sexual proportion and length structure. For instance, the establishment of a long-term monitoring program can help to determine not only the dynamics of populations but also if they are in decline or stable. Conservation programs of threatened species require genetic and ecological actions that facilitate their recovery in natural habitat, since the elimination of a niche result in the local extinction of the using species (Frankham, Briscoe, & Ballou, 2002). Consequently, conservation plans should prioritize habitat restoration and conservation with the aim of expanding population ranges, patches of suitable habitat and increase population numbers. Furthermore, an ecological flow design can reduce the existent isolation due to hydrological and climatic conditions. Given the high degree of genetic structuring, the differentiation of conservation groups is of particular importance for this endangered species. Correct conservation plans should recognize the genetic independence of *A. sophiae* populations and manage separately preventing the loss of locally adapted genotypes; this is of particular concern if the development of a captive breeding program is necessary (Perdices et al., 2001).

ACKNOWLEDGEMENTS

We would like to thank Prof. Dr. G. Wörheide and Prof. Dr. B. Reichenbacher (LMU, Munich) for providing access to the Molecular Geo- and Palaeobiology Lab at LMU (Munich). Also special thanks to Prof. Dr. H. R. Esmaeili (Shiraz University, Iran) for kindly supporting field works from his grant, to Dr. R. Zarei (Alzahra University, Terhran), Dr. A. Gholamifard (Zahedan University, Iran), S. Babaei, B. Parsi, G. Sayadzadeh, S. Ghasemian, S. Mirghiasi and R. Zamanianejad for their kind help in fish collection, and to Prof. R. Melzer for providing access to the SEM at the Bavarian State Collection of Zoology (ZSM, Munich). CA also acknowledge support from CERCA Programme (Generalitat de Catalunya).

REFERENCES

Alcaraz, C., & García-Berthou, E. (2007). Life history variation of invasive mosquitofish (*Gambusia holbrooki*) along a salinity gradient. *Biological Conservation*, 139, 83–92. doi

Alcaraz, C., Pou-Rovira, Q., & García-Berthou, E. (2008*a*). Use of a flooded salt marsh habitat by an endangered cyprinodontid fish (*Aphanius iberus*). *Hydrobiologia*, 600, 177–185. doi

Alcaraz, C., Bisazza, A., & García-Berthou, E. (2008*b*). Salinity mediates the competitive interactions between invasive mosquitofish and an endangered fish. *Oecologia*, 155, 205–213. doi

Alcaraz, C., Carmona-Catot, G., Risueño, P., Perea, S., Pérez, C., Doadrio, I., & Aparicio, E. (2015*a*). Assessing population status of *Parachondrostoma arrigonis* (Steindachner, 1866), threats and conservation perspectives. *Environmental biology of fishes*, 98, 443–455. doi

Alcaraz, C., Gholami, Z., Esmaeili, H. R., & García-Berthou, E. (2015*b*). Herbivory and seasonal changes in diet of a highly endemic cyprinodontid fish (*Aphanius farsicus*). *Environmental Biology of Fishes*, 98, 1541–1554. doi

Ai, X. S., Sandoval-Solis, S., Dahlke, H. E., & Lane, B. A. (2015). Reconciling hydropower and environmental water uses in the Leishui River Basin. *River research and applications*, 31, 181–192. doi

Angeletti, D., Cimmaruta, R., & Nascetti, G. (2010). Genetic diversity of the killifish *Aphanius* *fasciatus* paralleling the environmental changes of Tarquinia salterns habitat. *Genetica*, 138, 1011–1021. doi

Angeletti, D., Sebbio, C., Carlini, A., Strinati, C., Nascetti, G., Carere, C., & Cimmaruta, R. (2017). The role of habitat choice in micro-evolutionary dynamics: An experimental study on the Mediterranean killifish *Aphanius fasciatus* (Cyprinodontidae). *Ecology and evolution*, 7, 10536–10545. doi

Bacha, M., Jeyid, A. M., Jaafour, S., Yahyaoui, A., Diop, M. & Amara, R. (2016). Insights on stock structure of round sardinella *Sardinella aurita* off north-west Africa based on otolith shape analysis. *Journal of fish biology*, 89, 2153–2166. doi

Bonato, L., Corbetta, A., Giovine, G., Romanazzi, E., Šunje, E., Vernesi, C., & Crestanello, B. (2018). Diversity among peripheral populations: genetic and evolutionary differentiation of *Salamandra atra* at the southern edge of the Alps. *Journal of Zoological Systematics and Evolutionary Research*, 56, 533–548. doi

Buonerba, L., Zaccara, S., Delmastro, G. B., Lorenzoni, M., Salzburger, W., & Gante, H. F. (2015). Intrinsic and extrinsic factors act at different spatial and temporal scales to shape population structure, distribution and speciation in Italian *Barbus* (Osteichthyes: Cyprinidae). *Molecular phylogenetics and evolution*, 89, 115–129. doi

Cabe, P. R., & Alstad, D. N. (1994). Interpreting population differentiation in terms of drift and selection. *Evolutionary Ecology*, 8, 489–492. doi

Casal-López, M., Perea, S., Sousa-Santos, C., Robalo, J. I., Torralva, M., Oliva-Paterna, F. J., & Doadrio, I. (2018). Paleobiogeography of an Iberian endemic species, *Luciobarbus sclateri* (Günther, 1868)(Actinopterygii, Cyprinidae), inferred from mitochondrial and nuclear markers. *Journal of Zoological Systematics and Evolutionary Research*, 56, 127–147. doi

Chiari, Y., Van Der Meijden, A., Mucedda, M., Lourenço, J. M., Hochkirch, A., & Veith, M. (2012). Phylogeography of Sardinian cave salamanders (genus *Hydromantes*) is mainly determined by geomorphology. *PLoS One*, 7, e32332. doi

Chiozzi, G., Stiassny, M. L., Alter, S. E., De Marchi, G., Mebrahtu, Y., Tessema, M., Asmamaw, B., Fasola, M., & Bellati, A. (2018). Fishes in the desert: mitochondrial variation and phylogeography of *Danakilia* (Actinopterygii: Cichlidae) and *Aphanius* (Actinopterygii: Cyprinodontidae) in the Danakil Depression of northeastern Africa. *Mitochondrial DNA Part A*, 29, 1025–1040. doi

Chung, M. Y., Nason, J. D., & Chung, M. G. (2005). Patterns of hybridization and population genetic structure in the terrestrial orchids *Liparis kumokiri* and *Liparis makinoana*

(Orchidaceae) in sympatric populations. *Molecular Ecology*, 14, 4389–4402. doi
Coad, B. W. (2018, August 30). Freshwater fishes of Iran. Retrieved from http://www.briancoad.com.
Díez-del-Molino, D., García-Berthou, E., Araguas, R. M., Alcaraz, C., Vidal, O., Sanz, N., & García-Marín, J. L. (2018). Effects of water pollution and river fragmentation on population genetic structure of invasive mosquitofish. *Science of the Total Environment*, 637, 1372–1382. doi
Faulks, L. K., Gilligan, D. M., & Beheregaray, L. B. (2011). The role of anthropogenic vs. natural in-stream structures in determining connectivity and genetic diversity in an endangered freshwater fish, Macquarie perch (*Macquaria australasica*). *Evolutionary Applications*, 4, 589–601. doi
Frankham, R., Briscoe, D. A., & Ballou, J. D. (2002). Introduction to conservation genetics. Cambridge university press.
Fullerton, A. H., Burnett, K. M., Steel, E. A., Flitcroft, R. L., Pess, G. R., Feist, B. E., Torgersen, C. E., Miller, D. J., & Sanderson, B. L. (2010). Hydrological connectivity for riverine fish: measurement challenges and research opportunities. *Freshwater biology*, 55, 2215–2237. doi
Fu, Y. X. (1997). Statistical tests of neutrality of mutations against population growth, hitchhiking and background selection. *Genetics*, 147, 915–925.
Gholami, Z., Teimori, A., Esmaeili, H. R., Schulz-Mirbach, T., & Reichenbacher, B. (2013). Scale surface microstructure and scale size in the tooth-carp genus *Aphanius* (Teleostei, Cyprinodontidae) from endorheic basins in Southwest Iran. *Zootaxa*, 3619, 467–490. doi
Gholami, Z., Esmaeili, H. R., Erpenbeck, D., & Reichenbacher, B. (2014). Phylogenetic analysis of *Aphanius* from the endorheic Kor River Basin in the Zagros Mountains, South-western Iran (Teleostei: Cyprinodontiformes: Cyprinodontidae). *Journal of Zoological Systematics and Evolutionary Research*, 52, 130–141. doi
Gholami, Z., Esmaeili, H. R., & Reichenbacher, B. (2015). New data on the zoogeography of *Aphanius sophiae* (Teleostei: Cyprinodontidae) in the Central Zagros (Southwest Iran). *Limnologica-Ecology and Management of Inland Waters*, 51, 70–82. doi
González E.G., Pedraza-Lara C. & Doadrio I. 2014. Genetic diversity and population history of the endangered killifish *Aphanius baeticus*. *Journal of Heredity*, 105, 597–610. doi
González, E. G., Cunha, C., Ghanavi, H. R., Oliva-Paterna, F. J., Torralva, M., & Doadrio, I. (2017). Phylogeography and population genetic analyses in the Iberian toothcarp (*Aphanius iberus* Valenciennes, 1846) at different time scales. *Journal of Heredity*, 109,

253–263. doi

Gutiérrez-Rodríguez, C., Morris, M. R., Dubois, N. S., & de Queiroz, K. (2007). Genetic variation and phylogeography of the swordtail fish *Xiphophorus cortezi* (Cyprinodontiformes, Poeciliidae). *Molecular phylogenetics and evolution*, 43, 111–123. doi

Haghighi, A. T., & Kløve, B. (2017). Design of environmental flow regimes to maintain lakes and wetlands in regions with high seasonal irrigation demand. *Ecological engineering*, 100, 120–129. doi

Huelsenbeck, J. P., & Ranala, B. (2004). Frequentist properties of Bayesian posterior probabilities of phylogenetic trees under simple and complex substitution models. *Systematic Biology*, 53, 904–913. doi

Irwin, D. M., Kocher, T. D., & Wilson, A. C. (1991). Evolution of the cytochrome *b* gene of mammals. *Journal of molecular evolution*, 32, 128–144. doi

Khan, S., & Sharma, V. (2010). Genetic differentiation and diversity analysis of medicinal tree *Syzygium cumini* (Myrtaceae) from ecologically different regions of India. *Physiology and Molecular Biology of Plants*, 16, 149–158. doi

Kottelat, M., & Freyhof, J. (2007). Handbook of European freshwater fishes. Publications Kottelat, Cornol, Switzerland, and Freyhof, Berlin, Germany.

Li, C., Bessert, M. L., Macrander, J., & Orti, G. (2009). Low variation but strong population structure in mitochondrial control region of the plains topminnow, *Fundulus sciadicus*. *Journal of fish biology*, 74, 1037–1048. doi

Marchio, E. A., & Piller, K. R. (2013). Cryptic diversity in a widespread live-bearing fish (Poeciliidae: *Belonesox*). *Biological Journal of the Linnean Society*, 109, 848–860. doi

Maltagliati, F., & Camilli, L. (2000). Temporal genetic variation in a population of *Aphanius fasciatus* (Cyprinodontidae) from a brackish-water habitat at Elba Island (Italy). *Environmental biology of fishes*, 57, 107–112. doi

Nadji, M. (1997). Rerouting of the Kor River from the Zagros Region into the Persian Gulf-a proposed solution to the problem of salinization in the Persepolis Basin, Iran. *Zeitschrift für Angewandte Geologie*, 43, 171–178.

Nafarzadegan, A. R., Vagharfard, H., Nikoo, M. R., & Nohegar, A. (2018). Socially-Optimal and Nash Pareto-Based Alternatives for Water Allocation under Uncertainty: an Approach and Application. *Water Resources Management*, 32, 2985–3000. doi

Nolf, D. (1985). Otolithi piscium. Handbook of paleoichthyology. Gustav Fischer, Stuttgart, New York.

Oromi, N., Valbuena-Ureña, E., Soler-Membrives, A., Amat, F., Camarasa, S., Carranza, S., Sanuy, D., & Denoël, M. (2019). Genetic structure of lake and stream populations in a Pyrenean amphibian (*Calotriton asper*) reveals evolutionary significant units associated with paedomorphosis. *Journal of Zoological Systematics and Evolutionary Research*, 57, 418–430. doi

Ouborg, N. J., Pertoldi, C., Loeschcke, V., Bijlsma, R. K., & Hedrick, P. W. (2010). Conservation genetics in transition to conservation genomics. *Trends in genetics*, 26, 177–187. doi

Perdices, A., Carmona, J. A., Fernández-Delgado, C., & Doadrio, I. (2001). Nuclear and mitochondrial data reveal high genetic divergence among Atlantic and Mediterranean populations of the Iberian killifish *Aphanius iberus* (Teleostei, Cyprinodotidae). *Heredity*, 87, 314–324. doi

Ramos-Onsins, S. E., & Rozas, J. (2002). Statistical properties of new neutrality tests against population growth. *Molecular Biology and Evolution*, 19, 2092–2100. doi

Reichenbacher, B., Sienknecht, U., Küchenoff, H., & Fenske, N. (2007). Combined otolith morphology and morphometry for assessing taxonomy and diversity in fossil and extant killifish (*Aphanius*, †*Prolebias*). *Journal of Morphology*, 268, 898–915. doi

Reichenbacher, B., Feulner, G. R., & Schulz-Mirbach, T. (2009). Geographic variation in otolith morphology among freshwater populations of Aphanius dispar (Teleostei, Cyprinodontiformes) from the southeastern Arabian Peninsula. Journal of Morphology, 270, 469–484. doi

Rosenthal, A., Coutelle, O., & Craxton, M. (1993). Large-scale production of DNA sequencing templates by microtitre format PCR. *Nucleic Acids Research*, 21, 173–174. doi

Rovira, A., Alcaraz, C., & Ibáñez, C. (2012). Spatial and temporal dynamics of suspended load at-a-cross-section: the lowermost Ebro River (Catalonia, Spain). *Water Research*, 46, 3671–3681. doi

Sheykhi, V., & Moore, F. (2012). Geochemical characterization of Kor River water quality, Fars Province, Southwest Iran. *Water Quality, Exposure and Health*, 4, 25–38. doi

Tajima, F. (1989). Statistical method for testing the neutral mutation hypothesis by DNA polymorphism. *Genetics*, 123, 585–595.

Teimori, A., Esmaeili, H. R., Hamidan, N., & Reichenbacher, B. (2018). Systematics and historical biogeography of the *Aphanius dispar* species group (Teleostei: Aphaniidae) and description of a new species from Southern Iran. *Journal of Zoological Systematics and Evolutionary Research*, 56, 579–598. doi

Templeton, A. R., Crandall, K. A., & Sing, C. F. (1992). A cladistic analysis of phenotypic associations with haplotypes inferred from restriction endonuclease mapping and DNA sequence data. III. Cladogram estimation. *Genetics*, 132, 612–633.

Vargas, S., Schuster, A., Sacher, K., Büttner, G., Schätzle, S., Läuchli, B., Hall, K., Hooper, J. N. A., Erpenbeck, D., & Wörheide, G. (2012). Barcoding Sponges: An Overview Based on Comprehensive Sampling. *PLoS ONE*, 7, e39345. doi

Wright, S. (1978). Evolution and the genetics of populations, Vol. IV. Variability within and among natural populations. University of Chicago Press, Chicago.

Young, A., Boyle, T., & Brown, T. (1996). The population genetic consequences of habitat fragmentation for plants. *Trends in ecology & evolution*, 11, 413–418. doi

Figure captions

FIGURE 1. Location of the sampling sites (red points) in the study area. SA: Safashahr; GH: Ghadamgah; DE: Denjan; MA: Maloosjan; KA: Kamjan; GM: Gomban; MO: Mohammadabad.

FIGURE 2. a) Example of SEM micrograph of *A. sophiae* left otolith; the otolith corresponds to a male from Ghadamgah. b) Otolith terminology following Nolf (1985); and c) otolith morphometric characters measured: excisura angle (E), posterior angle (P), posteroventral angle (PV), maximum length (l – l'), maximum height (h – h'), medial part length (m – m'), rostrum length (rl – l), rostrum height (r – m), antirostrum length (al – d), antirostrum height (m – a), dorsal part length (d – d').

FIGURE 3. Maximum likelihood (ln likelihood = –4688.5153, $\alpha = 0.3110$) phylogenetic tree of *A. sophiae* populations, from the Kor Basin, based on Cyt *b* gene sequences with other Iranian and Mediterranean *Aphanius* species as outgroups. Numbers on the left are bootstrap support values for maximum-likelihood, and numbers on the right are Bayesian likelihood values. GenBank accession numbers are shown. See also Figure 1 for geographic location of the populations analyzed. Summary of apomorphic changes in Cyt *b* gene sequence is provided in Supporting Information Table S3.

FIGURE 4. Statistical parsimony haplotype network of *A. sophiae* populations based on Cyt *b* gene sequences. Circle area is proportional to the haplotype frequency. Lines linking haplotypes corresponds to one mutational step, and small white dots indicate missing haplotypes. See also Figure 1 for geographic location of the populations analyzed. Summary of apomorphic changes in Cyt *b* gene sequence is provided in Supporting Information Table S3.

FIGURE 5. ANCOVAs size-adjusted means of otolith morphometric variables per *A. sophiae* population. ANCOVA adjusted means are the population means after adjusting for fish length. Bars are standard errors.

FIGURE 6. Stepwise CDA plot for the otolith morphometric variables of *A. sophiae* populations from the Kor Basin.

TABLE 1. Features of the sampling sites. SL is the standard length and SD is the standard deviation. The individuals from Maloosjan spring have been previously used in Gholami et al., (2014). See Figure 1 for location of the sampling sites.

Site	Location	Latitude Longitude	Altitude (m)	N Total	ZM-CBSU-ZG Code	SL Range Min–Max (mm)	SL Mean ± SD (mm)	Cyt *b* Analysed Individuals Accession numbers
	Safashahr	30º 34' 50.8" N		♂: 14		♂: 21.2–29.6	♂: 25.4 ± 2.3	GenBank: KJ634159–KJ634167; *N* = 9
SA	Spring-stream	53º 31' 51.7" E	2557	♀: 12	191–214, 267, 268	♀: 22.2–33.7	♀: 26.4 ± 3.1	ZM-CBSU-ZG: 192, 193, 201, 202, 207–211
	Ghadamgah	30º 15' 23.0" N		♂: 10		♂: 17.8–29.3	♂: 23.2 ± 3.0	GenBank: KJ634168–KJ634175; *N* = 8
GH	Spring-stream	52º 24' 36.4" E	1660	♀: 10	25–39, 126–130	♀: 20.9–38.8	♀: 25.6 ± 5.4	ZM-CBSU-ZG: 126–130, 33, 34, 39
	Denjan	29º 57' 50.9" N		♂: 13		♂: 20.6–33.2	♂: 26.6 ± 4.2	GenBank: KJ634176–KJ634182; *N* = 7
DE	Spring-stream	52º 24' 12.5" E	1630	♀: 12	215–238, 373	♀: 21.3–38.1	♀: 31.5 ± 6.2	ZM-CBSU-ZG: 217, 220, 221, 226, 227, 229, 232
	Maloosjan	29º 52' 19.7" N		♂: 6		♂: 24.7–35.6	♂: 30.1 ± 4.6	GenBank: KF559215–KF559222; *N* = 8
MA	Spring-stream	52º 29' 48.4" E	1656	♀: 8	177–190	♀: 23.7–42.8	♀: 31.7 ± 6.5	ZM-CBSU-ZG: 178–182, 184, 185, 187
	Kamjan	29º 40' 19.5" N		♂: 13		♂: 21.9–26.8	♂: 24.1 ± 1.2	GenBank: KJ634183–KJ634190; *N* = 8
KA	Spring-stream	53º 09' 26.6" E	1571	♀: 10	143–160, 174–176, 244	♀: 17.8–30.3	♀: 27.0 ± 3.6	ZM-CBSU-ZG: 147, 150, 154, 156, 157, 159, 174, 244
	Gomban	29º 47' 48.4" N		♂: 12		♂: 18.5–27.2	♂: 23.3 ± 2.6	GenBank: KJ634191–KJ634197; *N* = 7
GM	Spring-stream	53º 28' 57.9" E	1558	♀: 11	77–97, 131, 240–241	♀: 15.4–35.3	♀: 22.6 ± 7.2	ZM-CBSU-ZG: 91–93, 242, 243
	Mohammadabad	29º 14' 50.7" N		♂: 7		♂: 23.9–33.2	♂: 28.8 ± 3.6	GenBank: KJ634198–KJ634206; *N* = 9
MO	Spring-stream	53º 59' 06.5" E	1591	♀: 6	161–173	♀: 25.2–34.2	♀: 29.3 ± 3.2	ZM-CBSU-ZG: 162–165, 167, 169, 170–172

TABLE 2. Genetic diversity inferred from Cyt *b* sequences in studied populations. *N*, number of samples successfully analyzed; *S*, number of segregating sites; *h*, number of haplotypes; h_u, number of unique haplotypes; *H*, haplotype diversity; *π*, nucleotide diversity; *k*, average number of nucleotide differences.

Population	**Code**	***N***	***S***	***h***	h_u	***H***	***k***	***π***	**Tajima's *D***	**Fu's *Fs***
Pooled		56	34	21		0.91623	5.04740	0.00612	-1.05270[a]	-5.14582[a]
Safashahr	SA	9	0	1	1	0.00000	0.00000	0.00000	*npd*	*npd*
Ghadamgah	GH	8	2	2	2	0.42857	0.85714	0.00104	0.41421[ns]	1.65331[ns]
Denjan	DE	7	1	2	1	0.28571	0.28571	0.00035	-1.00623[ns]	-0.09474[ns]
Maloosjan	MA	8	2	3	2	0.60714	0.78571	0.00095	0.06935[ns]	-0.22360[ns]
Kamjan	KA	8	13	6	6	0.89286	4.53571	0.00550	-0.48282[ns]	-0.68914[ns]
Gomban	GM	7	10	7	7	1.00000	2.85714	0.00346	-1.60974[b]	-4.55660[c]
Mohammadabad	MO	9	0	1	1	0.00000	0.00000	0.00000	*npd*	*npd*

npd, no polymorphisms detected; *ns*, not significant; *a*, $P < 0.05$; *b*, $P = 0.015$; *c*, $P = 0.001$

TABLE 3. Among-populations genetic differentiation of *Aphanius sophiae* in the Kor Basin. Population pairwise F_{ST} (below diagonal), average number of pairwise differences between populations; P_{iXY} (above diagonal), and average number of pairwise differences within population, P_{iX} (diagonal elements), are shown. Significance based on 1000 permutations.

Population	**Code**	**SA**	**GH**	**DE**	**MA**	**KA**	**GM**	**MO**
Safashahr	SA	0.00000	5.53793^{a}	7.19769^{a}	7.81531^{a}	6.17325^{a}	4.45221^{a}	5.03055^{a}
Ghadamgah	GH	0.92730^{a}	0.85923	6.69075^{a}	7.30762^{a}	5.66695^{a}	3.94820^{a}	4.52566^{a}
Denjan	DE	0.98293^{a}	0.91134^{a}	0.28606	0.89420^{c}	7.32708^{b}	5.60344^{a}	6.18257^{a}
Maloosjan	MA	0.95288^{a}	0.88736^{a}	0.38827^{c}	0.78710	7.94490^{a}	6.21847^{a}	6.79867^{a}
Kamjan	KA	0.64788^{a}	0.52110^{a}	0.65211^{b}	0.66295^{a}	4.56856	4.07590^{ns}	5.15941^{a}
Gomban	GM	0.71396^{a}	0.54089^{a}	0.71862^{a}	0.71629^{a}	0.08281^{ns}	2.86733	3.44294^{a}
Mohammadabad	MO	1.00000^{a}	0.91096^{a}	0.98012^{a}	0.94581^{a}	0.57707^{a}	0.62614^{a}	0.00000

ns, not significant; *a*, $P < 0.00001$; *b*, $P < 0.001$; *c*, $P < 0.025$

TABLE 4. Hierarchical analysis of molecular variance (AMOVA) for *Aphanius sophiae* populations, based on Cyt *b* sequences.

Source of variation	***df***	**Sum of Squares**	**Variance Components**	**Percent Variation**	**Fixation Indices**	***P*-Value**
Without Grouping						
Among populations	6	108.55	2.1852	77.43		< 0.0001
Within populations	49	31.22	0.6370	22.57	Φ_{ST} = 0.7743	< 0.0001
Total	55	139.77	2.8221			
Two groups[a]						
Among groups	1	24.17	0.2581	8.80	Φ_{CT} =0.0880	0.0381
Among populations within groups	5	84.39	2.0374	69.48	Φ_{SC} =0.7618	< 0.0001
Within populations	49	31.21	0.6370	21.72	Φ_{ST} = 0.7828	< 0.0001
Total	55	139.77	2.9325			
Three groups[b]						
Among groups	2	67.82	1.2941	41.35	Φ_{CT} =0.4135	< 0.0001
Among populations within groups	4	40.73	1.1987	38.30	Φ_{SC} =0.6530	< 0.0001
Within populations	49	31.21	0.6370	20.35	Φ_{ST} = 0.7965	< 0.0001
Total	55	139.77	3.1298			
Five groups[a]						
Among groups	4	103.79	2.1293	70.98	Φ_{CT} =0.7098	0.0137
Among populations within groups	2	4.76	0.2336	7.79	Φ_{SC} =0.2683	< 0.0001
Within populations	49	31.21	0.6370	21.23	Φ_{ST} = 0.7877	< 0.0001
Total	55	139.77	2.9999			

a: MO + GM + KA, MA + DE + GH + SA
b: MO + GM + KA, MA + DE, GH + SA
c: MO, GM + KA, MA + DE, GH, SA

TABLE 5. Percentage of correct classifications derived from a stepwise CDA for population identification of *Aphanius sophiae*, from the Kor Basin, based on selected otolith morphometric characters. N_t is the total number of otoliths analysed per population and *n* is the number of correct classified individuals.

			Predicted Population Membership													
			SA		**GH**		**DE**		**MA**		**KA**		**GM**		**MO**	
Population	**Code**	N_t	***n***	**%**	***n***	**%**	***n***	**%**	***n***	**%**	***n***	**%**	***n***	**%**	***n***	**%**
Safashahr	SA	26	26	100.0	0	0.0	0	0.0	0	0.0	0	0.0	0	0.0	0	0.0
Ghadamgah	GH	20	0	0.0	14	70.0	4	20.0	0	0.0	1	5.0	1	5.0	0	0.0
Denjan	DE	25	0	0.0	0	0.0	15	60.0	1	4.0	6	24.0	2	8.0	1	4.0
Maloosjan	MA	14	0	0.0	1	7.1	7	50.0	6	42.9	0	21.4	0	0.0	0	0.0
Kamjan	KA	23	0	0.0	1	4.3	0	0.0	0	0.0	19	82.6	2	8.7	1	4.3
Gomban	GM	23	0	0.0	2	8.7	2	8.7	0	0.0	0	0.0	18	78.3	1	4.3
Mohammadabad	MO	13	0	0.0	0	0.0	0	0.0	0	0.0	0	0.0	0	0.0	13	100.0

Figure 1. MS Alcaraz & Gholami

794

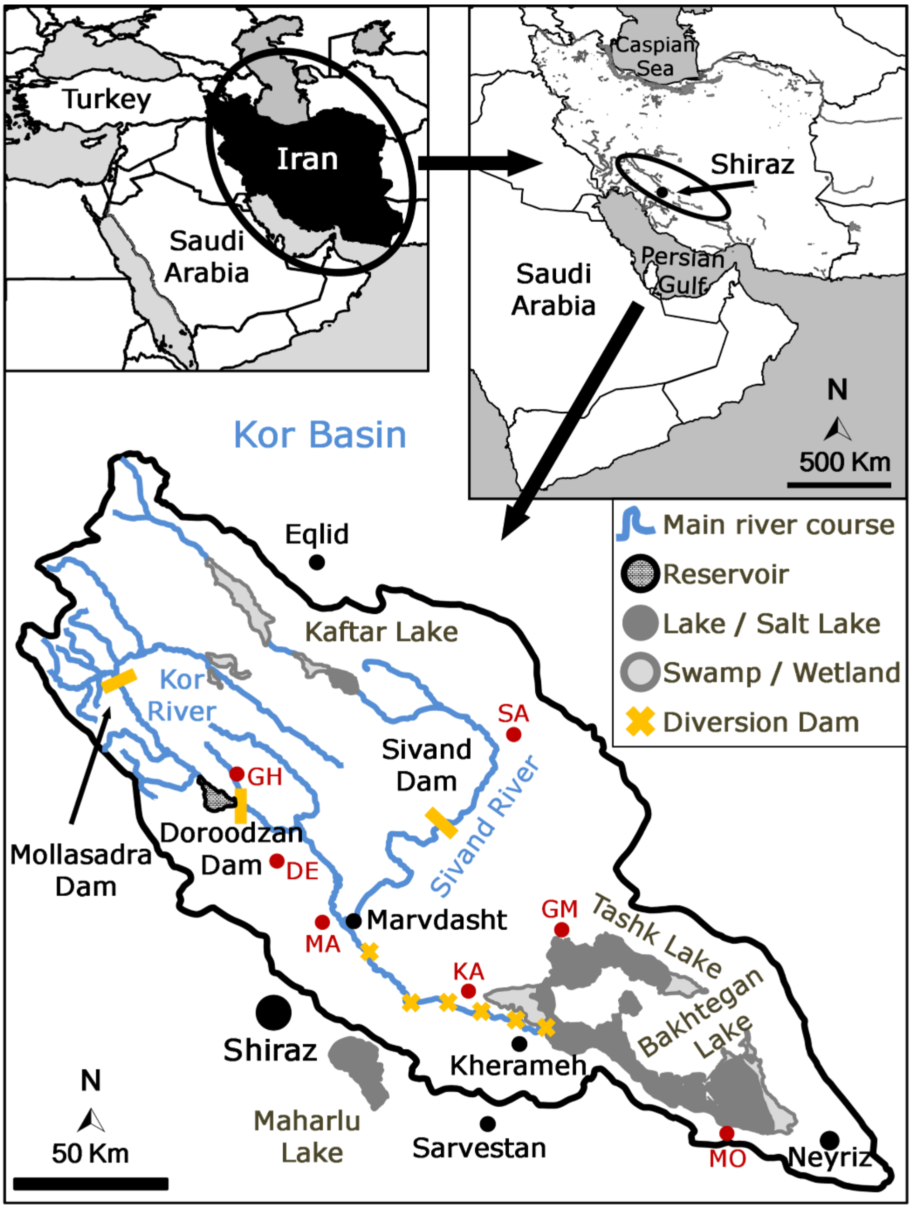

795

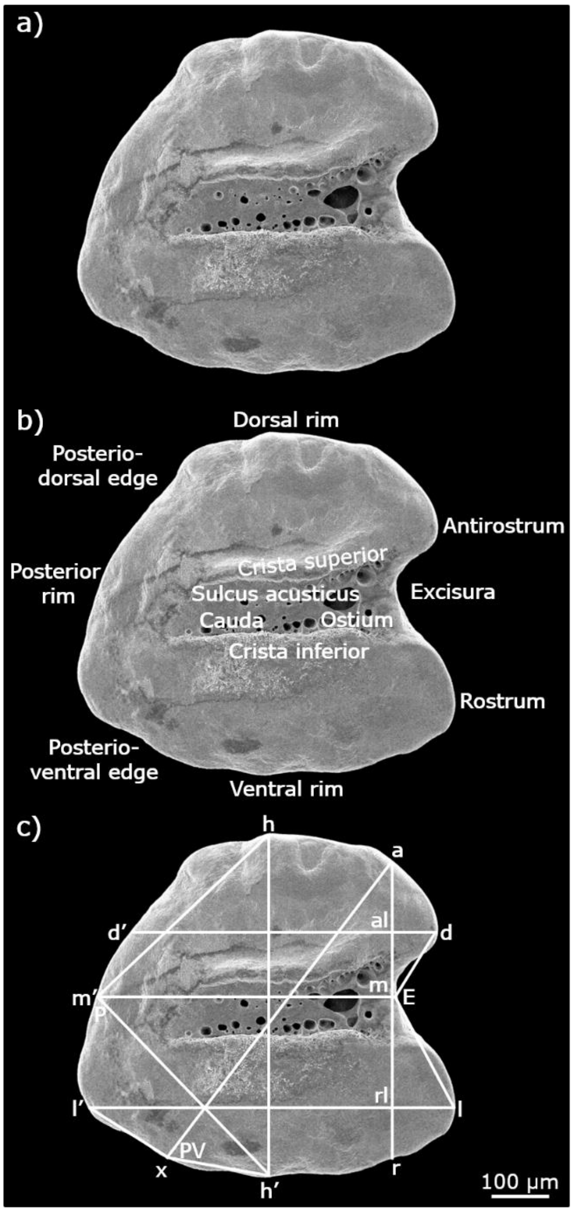
a)
b)
Dorsal rim
Posterio-
dorsal edge
Antirostrum
Posterior
rim
Crista superior
Sulcus acusticus
Excisura
Cauda
Ostium
Crista inferior
Rostrum
Posterio-
ventral edge
Ventral rim
c)
h
a
d'
al
d
m'
m
E
P
l'
rl
l
PV
x
h'
r
100 µm

Figure 3. MS Alcaraz & Gholami

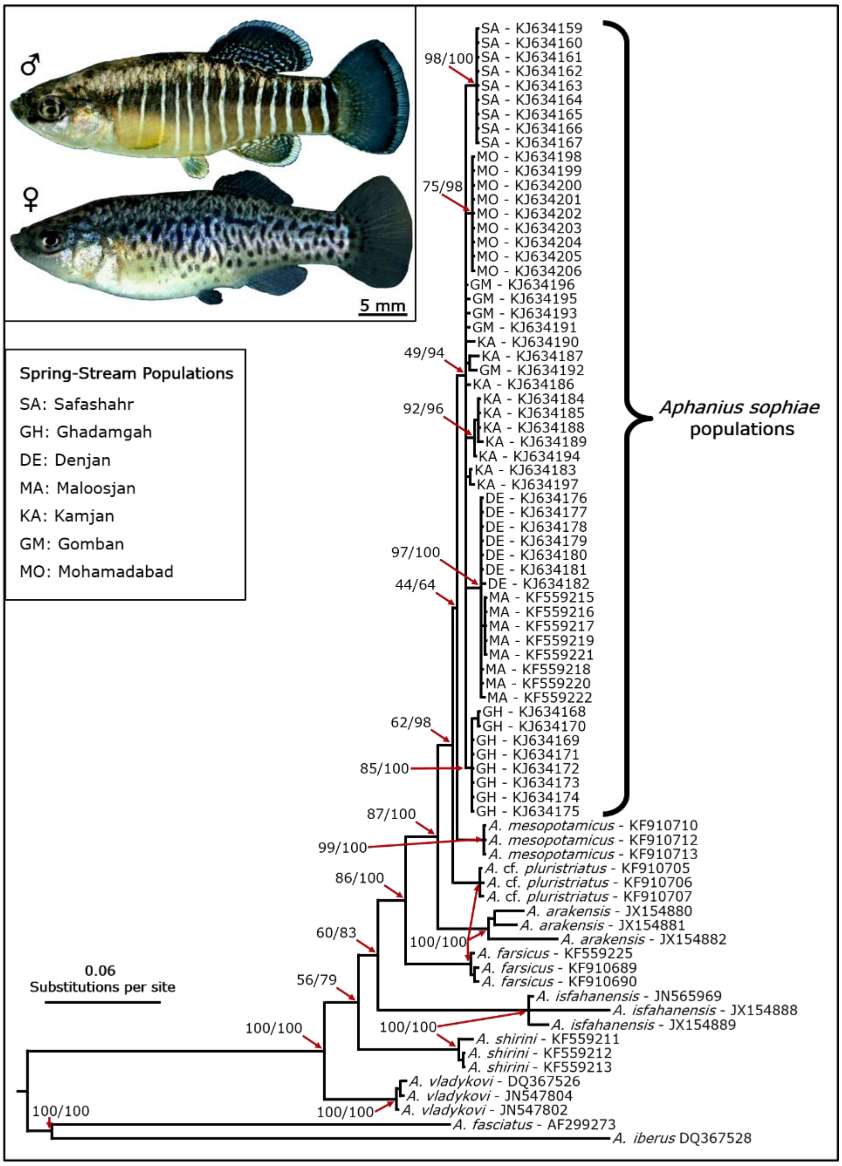

Figure 4. MS Alcaraz & Gholami

797

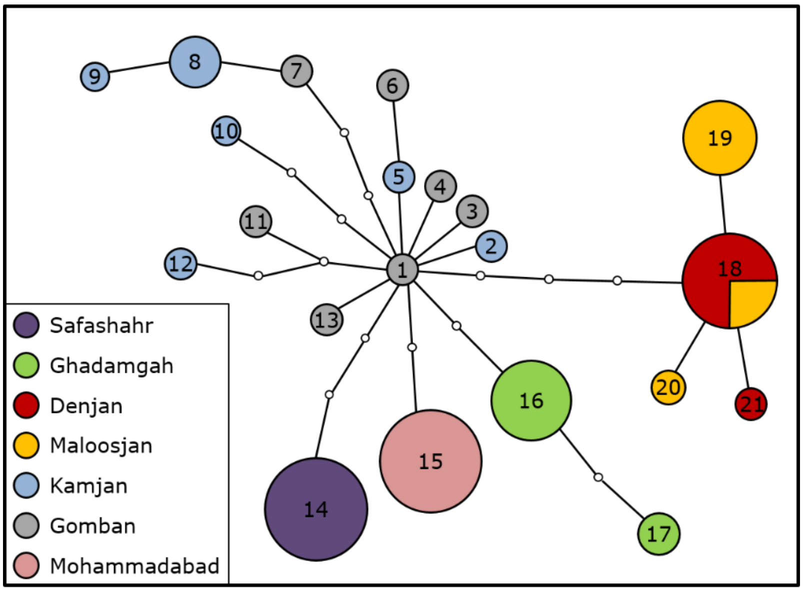

798

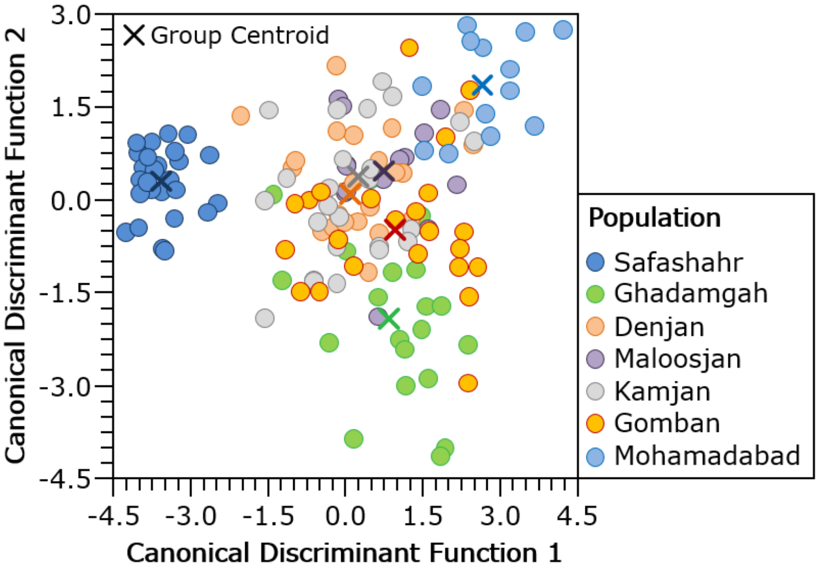
Group Centroid
Canonical Discriminant Function 2
3.0
1.5
0.0
-1.5
-3.0
-4.5
-4.5
-3.0
-1.5
0.0
1.5
3.0
4.5
Canonical Discriminant Function 1
Population
Safashahr
Ghadamgah
Denjan
Maloosjan
Kamjan
Gomban
Mohamadabad

799

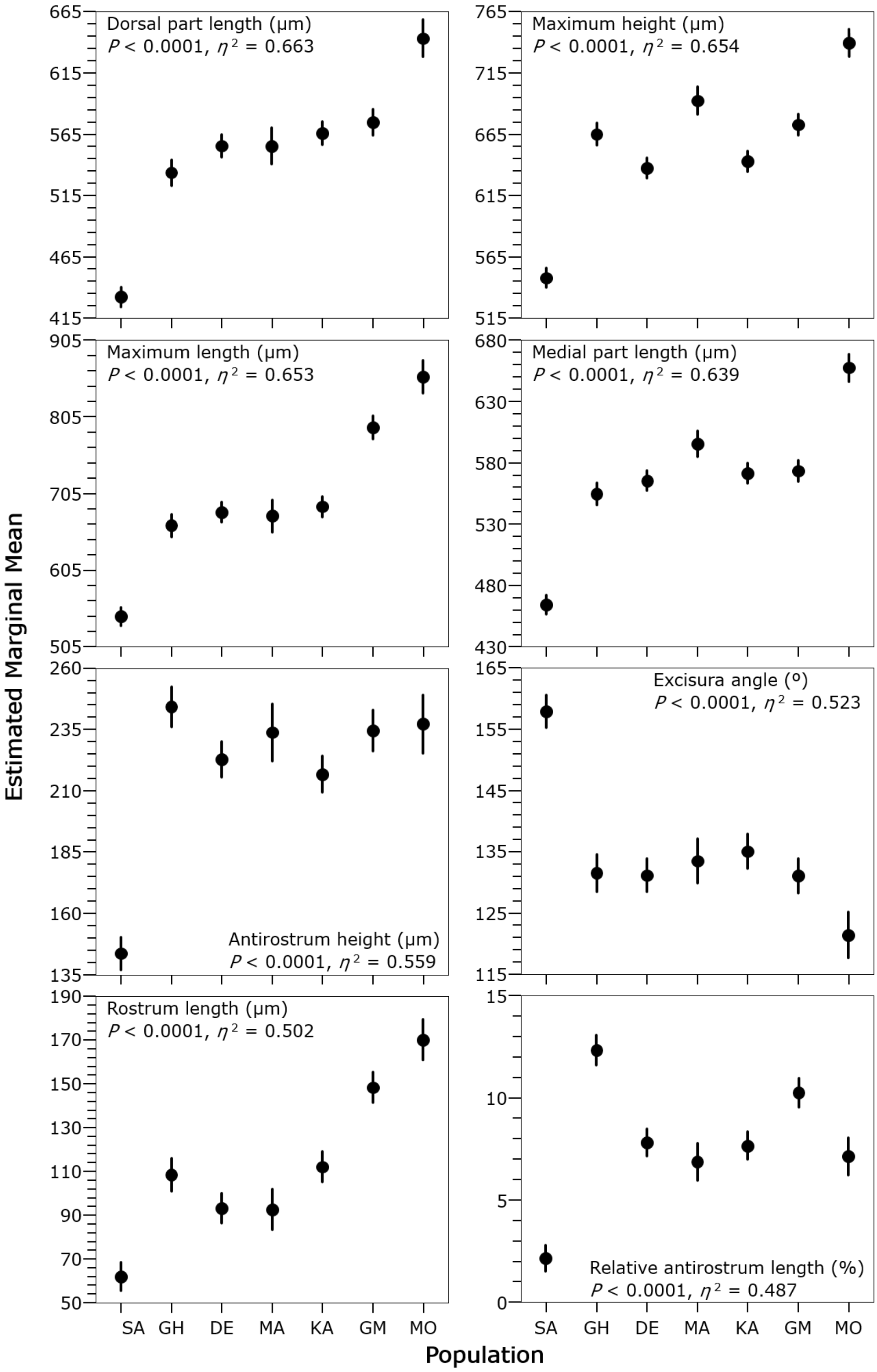

Dorsal part length (μm)
P < 0.0001, η^2 = 0.663
Maximum height (μm)
P < 0.0001, η^2 = 0.654
Maximum length (μm)
P < 0.0001, η^2 = 0.653
Medial part length (μm)
P < 0.0001, η^2 = 0.639
Antirostrum height (μm)
P < 0.0001, η^2 = 0.559
Excisura angle (°)
P < 0.0001, η^2 = 0.523
Rostrum length (μm)
P < 0.0001, η^2 = 0.502
Relative antirostrum length (%)
P < 0.0001, η^2 = 0.487
Estimated Marginal Mean
SA GH DE MA KA GM MO
Population

Electronic supplementary material to "**Diversity and structure of fragmented populations of a threatened endemic cyprinodontid (*Aphanius sophiae*) inferred from genetics and otolith morphology: implications for conservation and management**"

Carles Alcaraz and Zeinab Gholami

List of Figures and Tables.

FIGURE S1. Left otoliths SEM micrographs (in medial view) of *A. sophiae* populations from the Kor Basin. Three representative males and females are shown. Fish standard length (SL) in mm is given below each otolith.

FIGURE S2. ANCOVAs size-adjusted means of otolith morphometric variables per *A. sophiae* population. ANCOVA adjusted means are the population means after adjusting for fish length. Bars are standard errors.

TABLE S1. GenBank accession numbers for the outgroup Cyt *b* sequences included in the genetic analysis.

TABLE S2. Otolith morphometric variables measured (see Figure 2) and derived variables.

TABLE S3. Summary of the fixed apomorphic molecular genetic characters of the examined *Aphanius shopiae* populations from the Kor Basin, based on Cyt *b* gene sequences. Apomorphies are shared derived traits phylogenetically informative. Numbers above characters indicate the character position in the complete molecular genetic character matrix.

TABLE S4. Geographic distance (km) between populations of Aphanius sophiae in the Kor Basin. Euclidean distance (above diagonal), and hydrological (along river network) measured distance (below diagonal). The distance along the river network between *Aphanius* population was measured using the Network Analyst tool in ArcMap 10.5 (ESRI Inc., Redlands, CA, USA).

TABLE S5. Main features of the population otoliths studied per fish size class. Otolith range, mean (μ) and Standard deviation (SD) are shown. *N* is the number of otoliths examined, and SL is the fish standard length in mm.

TABLE S6. Range summary (minimum – maximum) of the otolith morphometric characters of *Aphanius sophiae* populations from the Kor Basin.

TABLE S7. Summary (mean ± standard deviation) of the otolith morphometric characters of *Aphanius sophiae* populations from the Kor Basin.

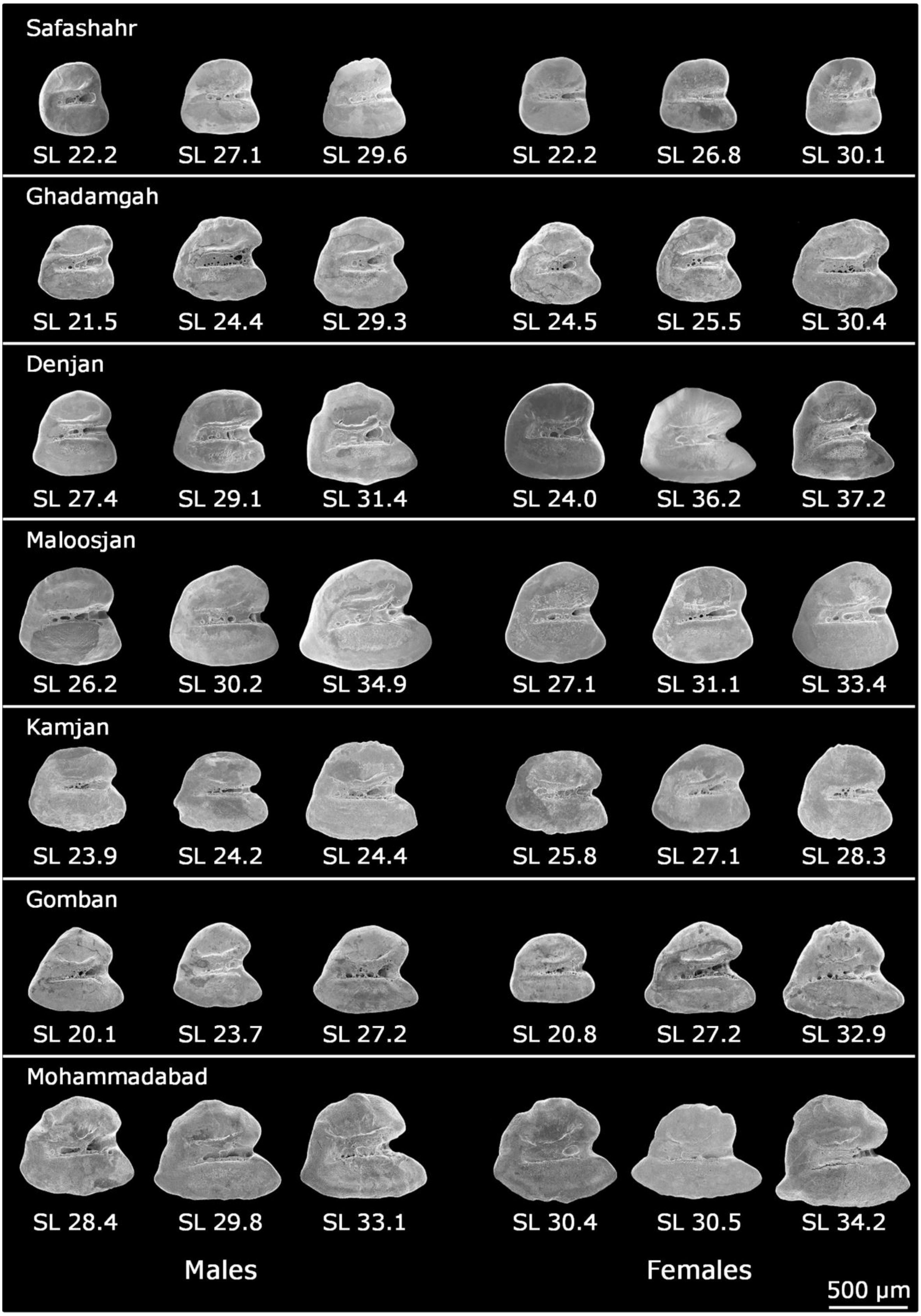

FIGURE S1. ANCOVAs size-adjusted means of otolith morphometric variables per *A. sophiae* population. ANCOVA adjusted means are the population means after adjusting for fish length. Bars are standard errors.

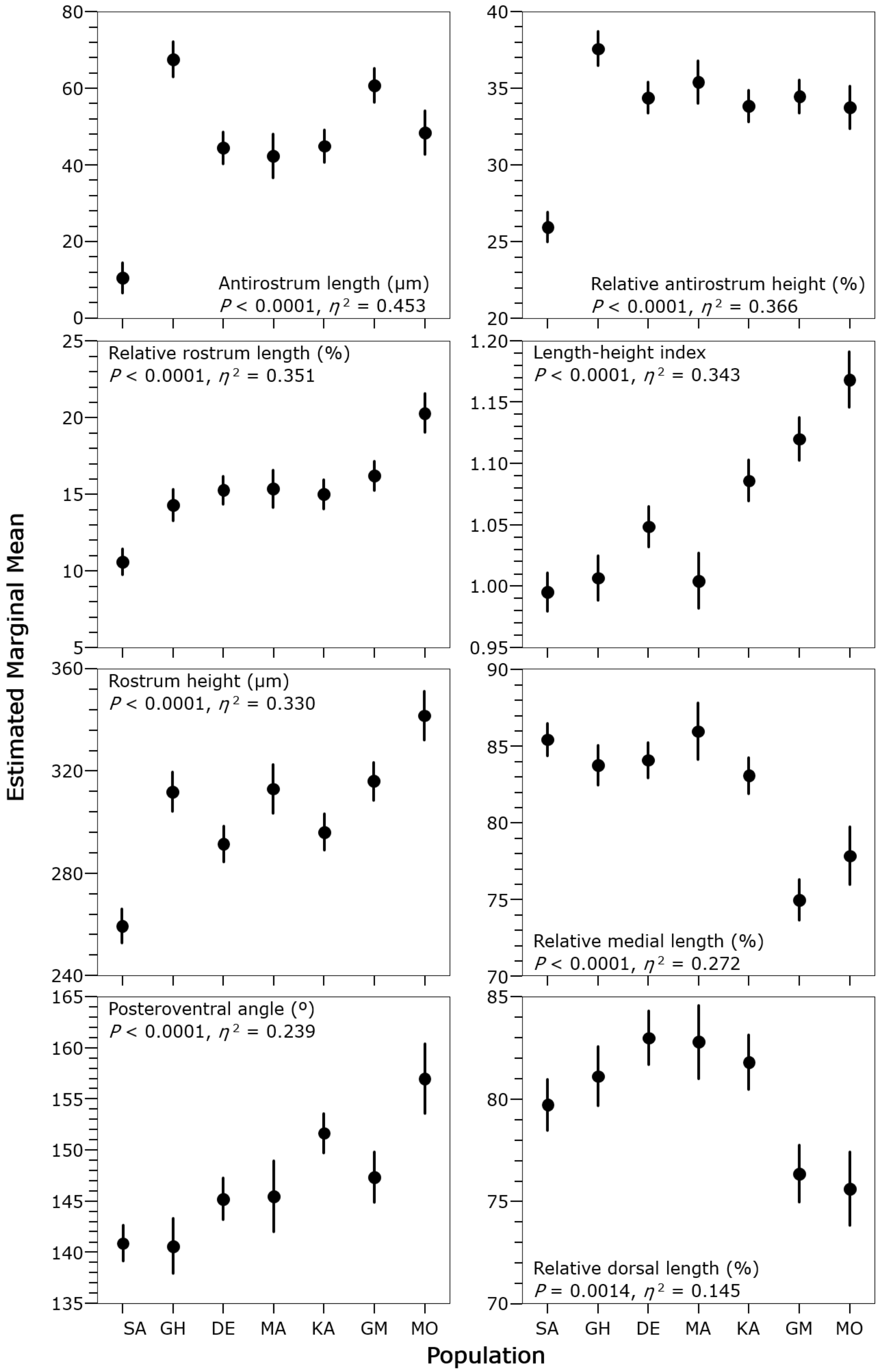

Figure S2. Left otoliths SEM micrographs (in medial view) of *A. sophiae* populations from the Kor Basin. Three representative males and females are shown. Fish standard length (SL) in mm is given below each otolith.

TABLE S1. GenBank accession numbers for the outgroup sequences included in the genetic analysis.

Species	*N*	GenBank Accession numbers	Locality, Country
Aphanius shirini	3	KF559211, KF559212, KF559213	Paselari spring, Iran
Aphanius cf. *pluristriatus*	3	KF910705, KF910706, KF910707	Khonj spring, Iran
Aphanius mesopotamicus	3	KF910710, KF910712, KF910713	Jarahi River, Iran
Aphanius arakensis	3	JX154880, JX154881, JX154882	Namak Lake Basin, Iran
Aphanius farsicus	3	KF559225, KF910689, KF910690	Barmeshoor spring, Iran
Aphanius isfahanensis	3	JN565969, JX154888, JX154889	Varzaneh spring, Iran
Aphanius vladykovi	3	DQ367526, JN547802, JN547804	Chaghakhor Wetland, Iran
Aphanius fasciatus	1	AF299273	Klisova Marshes, Greece
Aphanius iberus	1	DQ367528	Santa Pola, Spain

TABLE S2. Otolith morphometric variables measured (see Fig. 2) and derived variables.

Morphometric Variable	Description
Measured variables	
Excisura angle (º)	E
Posterior angle (º)	P
Posteroventral angle (º)	PV
Dorsal part length (µm)	d – d'
Maximum length (µm)	l – l'
Maximum height (µm)	h – h'
Medial part length (µm)	m – m'
Antirostrum length (µm)	al – d
Antirostrum height (µm)	m – a
Rostrum length (µm)	rl – l
Rostrum height (µm)	r – m
Derived variables	
Relative maximum length (%)	(maximum length / fish standard length (in µm)) × 100
Length-height index	maximum length / maximum height
Relative dorsal length (%)	(dorsal part length / maximum length) × 100
Relative medial length (%)	(medial part length / maximum length) × 100
Relative rostrum length (%)	(rostrum length / maximum length) × 100
Relative rostrum height (%)	(rostrum height / maximum height) × 100
Relative antirostrum length (%)	(antirostrum length / dorsal part length) × 100
Relative antirostrum height (%)	(antirostrum height / maximum height) × 100

TABLE S3. Summary of the fixed apomorphic molecular characters of the examined *Aphanius shopiae* populations from the Kor Basin, based on Cyt *b* gene sequences. Apomorphies are shared derived traits phylogenetically informative. Numbers above characters indicate the character position in the complete molecular character matrix.

		Position													
Population	**Code**	0130	0232	0403	0427	0481	0559	0574	0604	0718	0865	0883	1030	1033	1105
Safashahr	SA	A	A	C	G	C	T	T	G	A	T	G	G	A	A
Ghadamgah	GH	A	A	T	G	T	T	T	G	G	T	G	A	G	C
Denjan	DE	G	T	C	A	T	C	T	C	G	C	G	G	G	C
Maloosjan	MA	G	T	C	A	T	C	T	C	G	C	G	G	G	C
Kamjan	KA	A	A	C	G	T	T	T	G	G	T	G	G	G	C
Gomban	GM	A	A	C	G	T	T	T	G	G	T	G	G	G	C
Mohammadabad	MO	A	A	C	G	T	T	C	G	G	T	A	G	G	C

TABLE S4. Geographic distance (km) between populations of *Aphanius sophiae* in the Kor Basin. Euclidean distance (above diagonal), and hydrological (along river network) measured distance (below diagonal). The distance along the river network between *Aphanius* population was measured using the Network Analyst tool in ArcMap 10.5 (ESRI Inc., Redlands, CA, USA).

Population	Cod	SA	GH	DE	MA	KA	GM	MO
Safashahr	SA		80.25	86.67	84.62	81.56	75.00	159.18
Ghadamgah	GH	185.49		34.23	48.26	108.67	123.82	207.29
Denjan	DE	164.61	120.28		16.04	85.64	106.94	184.83
Maloosjan	MA	156.98	111.90	25.59		70.89	93.95	169.65
Kamjan	KA	169.65	125.19	100.62	93.09		29.73	99.38
Gomban	GM	223.56	179.10	154.53	147.00	53.91		86.40
Mohammadabad	MO	283.20	238.74	214.17	206.65	113.55	117.92	

TABLE S5. Main features of the population otoliths studied per fish size class. Otolith range, mean (***μ***) and Standard deviation (SD) are shown. *N* is the number of otoliths examined, and SL is the fish standard length in mm.

Population	**SC1 15 ≤ SL ≤ 20**			**SC2 20 < SL ≤ 27**			**SC3 27 < SL ≤ 35**			**SC4 35 < SL ≤ 43**		
	N	**Range**	***μ* ± SD**	***N***	**Range**	***μ* ± SD**	***N***	**Range**	***μ* ± SD**	***N***	**Range**	***μ* ± SD**
Otolith length (μm)												
Safashahr				20	441 – 582	519 ± 37	6	528 – 667	587 ± 52			
Ghadamgah	1	556	556	16	513 – 715	605 ± 63	2	698 – 809	754 ± 78	1	820	820
Denjan				9	524 – 693	604 ± 51	11	672 – 845	754 ± 67	5	750 – 931	866 ± 77
Maloosjan				4	577 – 736	652 ± 69	7	620 – 1035	798 ± 128	3	894 – 1147	998 ± 133
Kamjan	1	548	548	15	571 – 834	675 ± 82	7	632 – 754	692 ± 45			
Gomban	5	433 – 539	489 ± 43	12	434 – 806	669 ± 121	5	743 – 948	852 ± 88	1	1029	1029
Mohammadabad				4	759 – 882	816 ± 52	9	836 – 1085	974 ± 87			
Otolith length / SL (%)												
Safashahr				20	2.00 – 2.23	2.09 ± 0.07	6	1.80 – 2.16	2.01 ± 0.13			
Ghadamgah	1	3.12	3.12	16	2.26 – 2.90	2.60 ± 0.17	2	2.38 – 2.66	2.52 ± 0.20	1	2.11	2.11
Denjan				9	2.36 – 3.03	2.68 ± 0.21	11	2.05 – 2.95	2.49 ± 0.29	5	1.98 – 2.53	2.34 ± 0.24
Maloosjan				4	2.43 – 2.81	2.59 ± 0.16	7	2.22 – 2.97	2.57 ± 0.27	3	2.33 – 2.68	2.56 ± 0.20
Kamjan	1	3.08	3.08	15	2.38 – 3.42	2.78 ± 0.30	7	2.17 – 2.59	2.42 ± 0.14			
Gomban	5	2.52 – 2.91	2.69 ± 0.18	12	2.56 – 3.52	3.10 ± 0.27	5	2.54 – 3.36	2.98 ± 0.33	1	2.92	2.92
Mohammadabad				4	3.05 – 3.46	3.24 ± 0.18	9	2.76 – 3.57	3.17 ± 0.24			

TABLE S6. Range summary (minimum – maximum) of the otolith morphometric characters of *Aphanius sophiae* populations from the Kor Basin.

	Population						
	Safashahr	**Ghadamgah**	**Denjan**	**Maloosjan**	**Kamjan**	**Gomban**	**Mohammadabad**
N	26	20	25	14	23	23	13
SL (mm)	21.2 – 33.7	17.8 – 38.8	20.6 – 38.1	23.7 – 42.8	17.8 – 30.3	15.4 – 35.3	23.9 – 34.2
Excisura angle (º)	132 – 173	101 – 151	107 – 153	98 – 157	116 – 159	94 – 163	87 – 135
Posterior angle (º)	81 – 109	72 – 109	69 – 102	70 – 96	71 – 107	78 – 103	78 – 109
Posteroventral angle (º)	123 – 156	112 – 162	131 – 166	120 – 155	134 – 167	106 – 163	139 – 161
Dorsal part length (µm)	357 – 499	399 – 655	457 – 746	517 – 866	423 – 662	355 – 670	560 – 780
Maximum length (µm)	441 – 667	513 – 820	524 – 931	577 – 1147	548 – 834	433 – 1029	759 – 1085
Maximum height (µm)	476 – 597	499 – 800	533 – 859	625 – 911	519 – 743	452 – 790	621 – 888
Medial part length (µm)	377 – 516	442 – 657	478 – 727	516 – 857	463 – 643	383 – 692	568 – 758
Antirostrum length (µm)	1 – 47	7 – 114	15 – 106	10 – 156	4 – 79	8 – 118	29 – 126
Antirostrum height (µm)	83 – 215	169 – 321	138 – 296	186 – 411	134 – 292	136 – 299	187 – 362
Rostrum length (µm)	17 – 116	28 – 196	41 – 189	46 – 269	45 – 199	11 – 318	130 – 310
Rostrum height (µm)	174 – 313	216 – 387	232 – 396	261 – 465	235 – 396	155 – 400	282 – 439
Rel. maximum length (%)	1.80 – 2.23	2.11 – 3.12	1.98 – 3.03	2.22 – 2.97	2.17 – 3.42	2.52 – 3.52	2.76 – 3.57
Length-height-index	0.9095 – 1.1480	0.8479 – 1.1804	0.8836 – 1.2789	0.8945 – 1.2591	0.9678 – 1.25	0.8218 – 1.3025	1.0903 – 1.3486
Rel. dorsal length (%)	69.40 – 88.02	66.83 – 93.76	70.75 – 99.47	66.09 – 91.28	69.06 – 97.11	62.49 – 101.39	63.79 – 80.55
Rel. medial length (%)	74.81 – 92.82	73.91 – 94.74	74.51 – 91.64	68.79 – 92.21	70.14 – 93.90	59.77 – 103.23	65.49 – 82.39
Rel. rostrum length (%)	3.57 – 17.39	5.08 – 23.9	7.30 – 22.45	7.97 – 23.77	7.17 – 23.86	2.54 – 30.9	14.64 – 29.47
Rel. rostrum height (%)	33.92 – 54.37	38.37 – 54.98	40.61 – 52.72	38.73 – 53.26	38.28 – 56.14	34.29 – 53.65	39.64 – 50.14
Rel. antirostrum length (%)	0.23 – 9.42	1.75 – 19.93	3.07 – 16.07	1.73 – 18.01	0.95 – 12.23	2.02 – 18.35	4.31 – 16.22
Rel. antirostrum height (%)	16.47 – 38.32	27.21 – 44.49	21.46 – 42.68	26.88 – 45.12	20.46 – 45.76	25.68 – 45.01	27.3 – 42.04

TABLE S7. Summary (mean ± standard deviation) of the otolith morphometric characters of *Aphanius sophiae* populations from the Kor Basin.

	Population						
	Safashahr	**Ghadamgah**	**Denjan**	**Maloosjan**	**Kamjan**	**Gomban**	**Mohammadabad**
N	26	20	25	14	23	23	13
SL (mm)	25.85 ± 2.68	24.40 ± 4.42	28.94 ± 5.73	31.01 ± 5.55	25.33 ± 2.86	22.97 ± 5.21	29.02 ± 3.29
Excisura angle (º)	158 ± 9	132 ± 13	131 ± 13	134 ± 17	135 ± 11	131 ± 18	121 ± 14
Posterior angle (º)	92 ± 6	89 ± 10	90 ± 7	86 ± 8	88 ± 9	91 ± 6	91 ± 10
Posteroventral angle (º)	141 ± 8	137 ± 11	146 ± 8	142 ± 8	151 ± 8	145 ± 12	154 ± 7
Dorsal part length (µm)	427 ± 36	513 ± 66	589 ± 91	637 ± 107	553 ± 55	521 ± 87	687 ± 72
Maximum length (µm)	535 ± 49	629 ± 88	723 ± 117	799 ± 165	675 ± 75	685 ± 172	925 ± 107
Maximum height (µm)	540 ± 33	635 ± 69	674 ± 87	759 ± 91	627 ± 55	622 ± 105	777 ± 74
Medial part length (µm)	458 ± 34	531 ± 59	594 ± 76	648 ± 92	559 ± 40	534 ± 82	687 ± 54
Antirostrum length (µm)	8 ± 10	60 ± 24	54 ± 27	60 ± 43	41 ± 19	48 ± 29	58 ± 32
Antirostrum height (µm)	140 ± 33	235 ± 36	236 ± 43	279 ± 65	211 ± 43	211 ± 51	268 ± 45
Rostrum length (µm)	57 ± 23	92 ± 39	113 ± 41	130 ± 70	103 ± 34	120 ± 70	191 ± 61
Rostrum height (µm)	255 ± 29	296 ± 49	311 ± 45	349 ± 57	287 ± 40	289 ± 69	361 ± 47
Rel. maximum length (%)	2.07 ± 0.09	2.60 ± 0.23	2.53 ± 0.28	2.57 ± 0.21	2.68 ± 0.31	2.97 ± 0.30	3.20 ± 0.21
Length-height-index	0.9904 ± 0.0542	0.9890 ± 0.0806	1.0708 ± 0.0920	1.0447 ± 0.1114	1.0762 ± 0.0729	1.0894 ± 0.1228	1.1906 ± 0.0750
Rel. dorsal length (%)	79.96 ± 4.72	82.02 ± 6.91	81.8 ± 5.83	80.65 ± 7.62	82.28 ± 5.91	77.91 ± 9.70	74.38 ± 4.11
Rel. medial length (%)	85.80 ± 4.66	85.03 ± 6.49	82.78 ± 4.82	82.22 ± 7.04	83.24 ± 5.3	80.06 ± 10.14	74.73 ± 5.76
Rel. rostrum length (%)	10.61 ± 3.67	14.29 ± 4.48	15.27 ± 3.74	15.35 ± 5.24	15.01 ± 3.48	16.21 ± 6.56	20.3 ± 4.42
Rel. rostrum height (%)	47.25 ± 4.87	46.44 ± 5.04	46.16 ± 2.84	45.91 ± 3.84	45.8 ± 4.38	45.88 ± 4.81	46.4 ± 3.02
Rel. antirostrum length (%)	1.90 ± 2.03	11.45 ± 3.98	8.86 ± 3.62	8.81 ± 5.01	7.18 ± 3.00	8.76 ± 4.73	8.25 ± 3.76
Rel. antirostrum height (%)	25.79 ± 5.4	37.07 ± 5.22	34.99 ± 4.43	36.53 ± 5.48	33.59 ± 6.00	33.65 ± 4.33	34.41 ± 3.5